Improving Antibiotic Physicochemical Properties using a Crystal Engineering Approach

Merve ARPACIOGLU

Thesis to obtain the Master of Science Degree in

Biotechnology

Supervisors: Professor Maria Teresa Nogueira Leal da Silva Leal Duarte

Doctor Vânia Mafalda de Oliveira André

Examination Committee

Chairperson: Professor Arsénio do Carmo Sales Mendes Fialho

Supervisor: Doctor Vânia Mafalda de Oliveira André

Members of Committee: Professor João Luís Alves Ferreira da Silva

July 2019

I declare that this document is an original work of my own authorship and that it fulfils all the requirements of the Code of Conduct and Good Practices of the *Universidade de Lisboa*.

To Mustafa Kemal ATATURK,

Who states, “In human life, you will find players of religion until the knowledge and proficiency in religion will be cleansed from all superstitions, and will be purified and perfected by the enlightenment of real science.”

Acknowledgements

First of all, I would like to thank Professor Maria Teresa Duarte for being part of her research group, enlarging my vision and knowledge and allowing me doing my MSc thesis throughout my Erasmus+ mobility action at Instituto Superior Tecnico.

Second of all, I would like to express my gratitude and special thanks to my mentor, Vania André, for her professional guidance, mentorship, dearest understanding, and countless help I have received, not only professionally but also with any problem occurred during my stay in Lisbon. This thesis could not have been made without her contributions.

Moreover, I would like to tell my special thanks for the whole Centro de Química Estrutural research group member who was also there for me with their professional help anytime. Additionally, I would like to express my special thanks to Auguste Fernandes for the TGA and DSC data.

Asides from that, I am extremely thankful to Prof. Dr. Gulsah Sanli Mohammed, who supported me for my mobility action in the first place.

Yet, my deepest gratitude goes to my beloved family members, Ibrahim Arpacioglu, Sevim Arpacioglu and Metin Arpacioglu, for their endless support and believe in me, which I have had during my entire life.

Last but not least, I am grateful to my friends from Turkey and Portugal and particularly my boyfriend, Domenico Bravo, for making my stay more delightful with his company and ever-lasting friendship.

Abstract

This study aims to expand the pharmaceutical solid-state forms of Sparfloxacin (SPX), an active pharmaceutical ingredient (API), by using crystal engineering principles. SPX is a fluorinated quinolone antibiotic withdrawn from the market because of its severe side effects. This drug offers a trade-off between high solubility and low membrane permeability due to its zwitterionic nature. So, the ultimate goal is to develop new multicomponent crystal forms of SPX with different physicochemical properties. After a polymorphic screening, the multicomponent forms of SPX are extended within this study by the use of 4- Aminosalicylic (4-ASA), 3-Aminobenzoic acid (3-ABA), Anthranilic acid (AA), and Nalidixic acid (NA) as co-formers. All the multicomponent forms obtained are salts formed between Sparfloxacin and the co-former, in which SPX always plays the cationic role. Also a solvate with acetonitrile was formed within these studies. The solubility of the multicomponent forms was improved compared with SPX owing to the salt nature of multicomponent forms. Lastly, the new multicomponent forms are stable under 78% humidity atmosphere. It is worth mentioning that a superior antimicrobial activity is expected in the salts of SPX with 4-ASA since both compounds are antibiotics and they have shown to be effective in the treatment of tuberculosis through different pahtways.

Keywords

Crystal engineering, supramolecular synthons, pharmaceutical crystal forms, Sparfloxacin

Resumo

Este estudo tem como objetivo utilizar os princípios da engenharia de cristais para aumentar o número de formas cristalinas da sparfloxacina (SPX) enquanto princípio farmacologicamente ativo (API). A SPX é um antibiótico da família das quinolonas que foi retirado do mercado devido aos seus efeitos secundários adversos. Devido à sua natureza zwitteriónica, este fármaco apresenta uma boa solubilidade, mas baixa permeabilidade nas membranas celulares. Assim, com este trabalho pretende-se desenvolver novas formas cristalinas multicomponentes de SPX com diferentes propriedades físico-químicas. Após um rastreio polimórfico, foram obtidas novas formas multicomponentes combinando SPX com os ácidos 4-aminosalicílico (4ASA), 3-aminobenzóico (3ABA), antranílico (AA) e nalidíxico (NA). Todas estas novas formas correspondem a sais, nos quais a SPX assume carga positiva. Foi ainda identificado um solvato com acetonitrilo. A solubilidade das novas formas cristalinas é superior à solubilidade da SPX, devido ao seu carácter de sal. Estas formas apresentam ainda uma boa estabilidade quando submetidas a uma atmosfera com 78% de humidade. Por fim, é importante mencionar que é expectável que os sais formados entre SPX e 4ASA tenham uma boa atividade antimicrobiana, uma vez que ambos os compostos são antibióticos eficazes no tratamento da tuberculese.

Palavras-chave

Engenharia de cristais, sintões supramoleculares, formas cristalinas de fármacos, Sparfloxacina

Table of Contents

List of Figures

List of Tables

List of Acronyms

API	Active Pharmaceutical Ingredient
SPX	Sparfloxacin
4-ASA	4-Aminosalicylic acid
3-ABA	3-Aminobenzoic acid
AA	Anthranilic acid
NA	Nalidixic acid
GRAS	Generally Regarded as Safe
SCXRD	Single Crystal X-ray Diffraction
PXRD	Powder X-ray Diffraction
FTIR	Fourier-transform Infrared Spectroscopy
FT-Raman	Fourier-transform Raman Spectroscopy
TGA	Thermogravimetric Analysis
DSC	Differential Scanning calorimetry
CSD	Cambridge Structural Database
ACN	Acetonitrile

List of Software

OriginPro 8	Data analysis and graphic software
Mercury 4.1.3	A software for 3D visualisation and exploration of crystal Packings
ConQuest 2.0.1	A software for searching and retrieving information from Cambridge Structural Database
DIFFRAC.COMMANDER	PXRD software
DIFFRAC.EVA V.5.0	PXRD software

Chapter 1

Introduction

1.1 Crystal Engineering and Supramolecular Chemistry

Crystal engineering, as defined by Desiraju,[1] is the field of 'understanding of intermolecular interactions in the context of crystal packing and utilization of such interactions in the design of new solids with desired physical and chemical properties'. Yet, the earliest use of the term of crystal engineering dates back to organic solid-state photochemistry studies done by G. M. J. Schmidt[2]. He concluded two key aspects of crystal engineering: the perception of crystals as self-assembly and molecular recognition as well as the relationship between molecular distribution within crystal lattice and physical and chemical properties of the material. Today, crystal engineering is regarded as a solid-state branch of supramolecular chemistry.[3]

In 1987, supramolecular chemistry was firstly introduced by Jean-Marie Lehn, a Nobel Prize winner, as the "chemistry beyond molecules".[4] As opposed to conventional chemistry fields, supramolecular chemistry is specialized in non-covalent interactions, for example hydrogen bonding, van der Waals forces, π-π interactions, and hydrophobic forces.

Over the time, various approaches have been offered in order to rationally design molecular crystals. Yet, one of the most widely applied and accepted approach is the supramolecular synthon approach, which was first revealed by Desiraju.[5]

1.2 Supramolecular Synthon Approach and Graph-set Analysis

"Crystal engineering is the new organic synthesis"

by Desiraju

Dunitz stated that the crystal is "a supermolecule par excellence[6]", as the assembly of molecules is governed by mutual recognition at an "amazing level of precision". Subsequently, based on this understanding, Desiraju redefinede crystal as "the *ultimate* example of supermolecule in that it consists of an infinity of molecule divergently bound".[5] He further intended to show the link between organic synthesis and crystal engineering as well as the similarities between conventional organic chemistry and molecular recognition e.g. hard soft acid and base principle.[5]

As it is named and used in supramolecular synthesis, the term synthon has been directly transferred into the crystal engineering field and used with its original meaning. The synthon was defined as "structural units within molecules which can be formed and/or assembled by known or conceivable synthetic operations" by Corey[7, 8]. Subsequently, Desiraju reduced the scope of the definition of supramolecular synthon and noted that "supramolecular synthons are structural units within supermolecules which can be formed and/or assembled by known or conceivable synthetic operations involving intermolecular interactions". Moreover, he also stated, "if crystals are the supramolecular

equivalents of molecules, crystal engineering is the supramolecular equivalent of organic synthesis". Yet, he also mentioned that the formation of supermolecules is not only governed by chemical factors but also, the geometrical factor is a great deal of matter.

To sum up, with a broad understanding, supramolecular synthons represent the possibility of molecular interactions, which leads to the formation of molecular assemblies of organic molecules, and Desiraju intended to show the relation between organic synthesis and crystal engineering with the hope of using extended knowledge of this branch of science. Furthermore, among exhaustive research, he concluded that there is higher probability of supramolecular interactions between specific organic functional groups in organic crystal molecules. The most common synthons can be found in the Cambridge Structural Database[9] (CSD), whilst offering the use of extended data sets that can be used as a guideline for the design of new crystal forms. The most commonly used supramolecular synthons in the co-crystal design can be found in Figure 1-1.

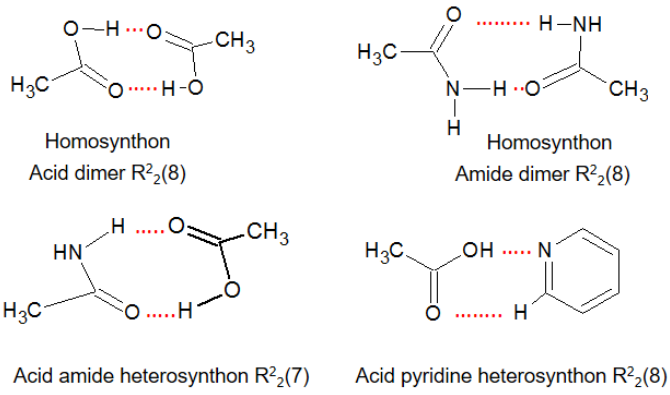

Figure 1-1 The most common supramolecular synthon used in the co-crystals[10]

Similar to supramolecular chemistry, the major tool of crystal engineering, in the subject of co-crystal design, relies on the use of hydrogen bonding. Hydrogen bonding was referred as the "master key for molecular recognition and the most reliable and directional interaction in supramolecular construction".[5]

There are basic hydrogen bonding rules for organic compounds, as stated by Etter,[11] which can be stated and generalized as follows:

1. All the good proton donors and acceptors are used in the hydrogen bonding;

2. Six-membered ring intermolecular interactions form in preference intermolecular hydrogen bonds;

3. The best proton donors and acceptors remaining after intramolecular hydrogen-bond formation form intermolecular hydrogen bonds to one another.

Asides the hydrogen bonding rules, Etter also brought the use of a mathematical method, graph-set theory, into the crystal engineering field in order to simplify hydrogen bonding patterns[12]. The notation of the graph-set theory is shown below:

$$G_d^a\ (n)$$

In this notation, *G* stands for the hydrogen bond motif. The possible hydrogen bond motifs denotations are:

- D: dimer or finite
- C: chain
- S: intermolecular
- R: ring

Additionally, the number of hydrogen acceptors is denoted *a*, whereas the number of hydrogen numbers is denoted *d*. Lastly, *n* represents the number of total atoms.

Nowadays, graph-set and supramolecular synthon theories are applied along with database mining using the Cambridge Structure Database[9] (CSD) for the design of novel multicomponent solids.

1.3 Solid-state forms in pharmaceutical science

In pharmaceutical science, the properties of the drug are highly related to the form of a given specific API. Along with various and diverse properties, APIs can be found in different forms like polymorphs, hydrates, solvates, salts, and co-crystals. Schematic representation of the multicomponent solid-state forms in pharmaceutical science is illustrated in Figure 1-2.

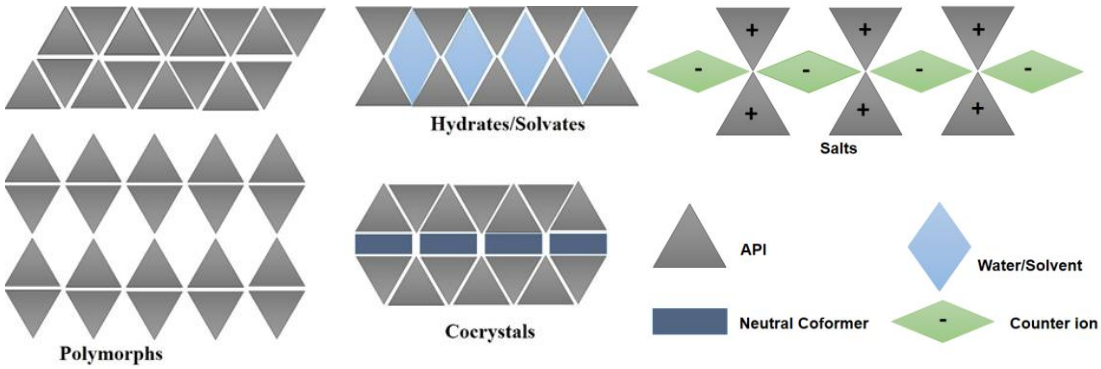

Figure 1-2 Schematic representation of the multicomponent solid-state forms in pharmaceutical science

Currently, it is remarkably important to be able to alter properties of the drug to enhance the behaviour and efficiency of the APIs utilized. Over the years, it has been shown that patentability and finding the

most efficient forms of drugs are parallel in the research devoted to this aim. For that reason there has been intense research regarding new forms of already known APIs, which is related to the crystal engineering field. Mostly common crystalline forms of pharmaceutical fields are mentioned below.

1.3.1 Polymorphism

Polymorphism refers to the tendency of compounds to exist in two or more crystalline forms whilst displaying the same chemical composition.[13] It is well-known that APIs are prone to have polymorphic forms due to the multiple active functional groups present in their chemical structures.[14] Since the crystal lattice structure differs in polymorphic forms, inevitably, its physicochemical properties vary as well.

There are two different kinds of polymorphisms: conformation polymorphism and packing polymorphism. Conformational polymorphism occurs when there is more than one conformation in the solid-state whereas packing polymorphism occurs when more than one packing arrangement is observed, caused by different supramolecular synthons, or they possess the same supramolecular synthons but display different crystal packing.

1.3.2 Solvate and hydrate

Solvate and hydrate forms of APIs are forms in which solvent molecules are incorporated within the lattice of APIs. In the case of solvent being water, the new form is called hydrate, in other cases, it is referred as solvate.[15] Particularly, hydrate's formation is common in APIs, because they have various functional groups that are capable of acting as either hydrogen acceptors or donors for water molecules. However, solid-state phase transitions, which can possibly change the physicochemical properties of the compounds, is a great deal of issues when it comes to hydrated forms of APIs.

1.3.3 Salt

Salt formation is the most widely applied technique in order to alter and improve the physicochemical properties of APIs in the pharmaceutical field. The main reason is the ease of the procedure. In general, salt formation is dependent on the presence of ionizable groups on the API because the principle behind the formation of salt is the ionic interaction between oppositely charged molecules. Therefore, salt formation is restricted to the presence of ionizable groups in APIs. Additionally, the formation of salts can only be achieved if there are at least two or three unit difference in p*K*a between the acid and the base.[16]

1.3.4 Co-crystal

Over the last few years, there have been many debates related to the definition of co-crystals. With its latest accepted version by FDA, pharmaceutical co-crystals can be defined as crystalline materials

composed of two or more different molecules, one of which is the API, in a defined stoichiometric ratio within the same crystal lattice that is associated with nonionic and noncovalent bonds.[17] In this respect, Generally Regarded As Safe (GRAS) molecules are combined with APIs for the formation of co-crystal within in a single crystal lattice.[18] Nowadays, co-crystallization is performed with the aim of improving the physicochemical properties such as stability, dissolution, and bioavailability of APIs.[19]

Furthermore, co-crystals can exist as hydrated or solvated forms likewise to APIs. The schematic of the co-crystal types is illustrated in Figure 1-3.

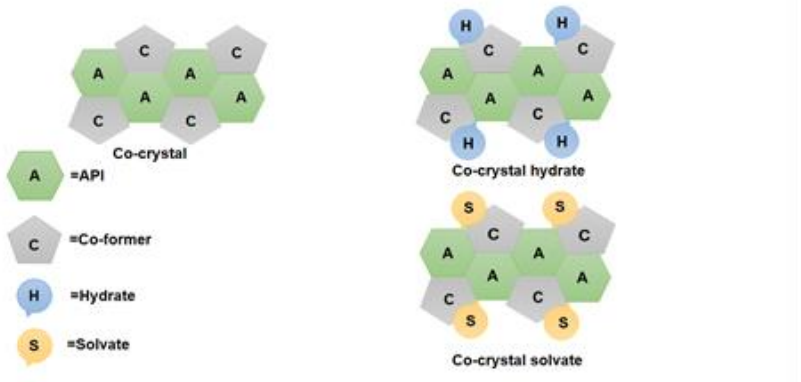

Figure 1-3 Schematic representation of co-crystal types[15]

Unlike other forms in the pharmaceutical field, co-crystal's formation has many advantages. To start with, the formation of co-crystal is not limited to the presence of ionizable functional groups as it is in salt formation. Instead, the formation is based on intermolecular interactions, e.g. hydrogen bonding (mostly used), hydrophobic forces, Van der Waals interactions etc. Hence, the possibility of obtaining a co-crystal form is hypothetically wider. Another advantage of co-crystals is that APIs are preserved rather than being changed. Apart from that, there are countless opportunities to form new crystal form, which can be designed with an enormous number of co-formers. Last but not least, co-crystals allow tailoring structural and physicochemical properties of APIs resulting in desired properties.[20, 21] Overall, designing co-crystal forms has become a priority by means of these advantages mentioned above.

Due to the relevance of co-crystals, they are going to be further detailed in the next section.

1.4 Co-crystal

1.4.1 History

In 1844, the discovery of the first co-crystal was made by Friedrich Wohler with the use of Quinone and hydroquinone.[22] Following this discovery, Pfeiffe stated that there were many established co-crystals

which can be classified into two groups: those ones composed of both inorganic and organic components, and the other ones composed only of with organic components in his book “Organische Molekulverbindungen[23]”.

On contrast to its long history, co-crystal, as a term, firstly became known in 1967, when it was used by Margret Etter.[11] Over the years, the influence of intermolecular interactions on packing of crystals, particularly hydrogen bonding, was better understood, hence, the rational design of co-crystals has become attention-grabbing, more specifically in the pharmaceutical industry because of its application possibility.[24]

1.4.2 Design of co-crystals and other multicomponent crystal forms

The design of co-crystals, as well as multicomponent crystal forms of APIs requires three stages: (1) the choice of API along with a suitable co-former, (2) supramolecular synthesis, and lastly (3) the characterization of the new form. The design stages are illustrated in the schematic shown below.

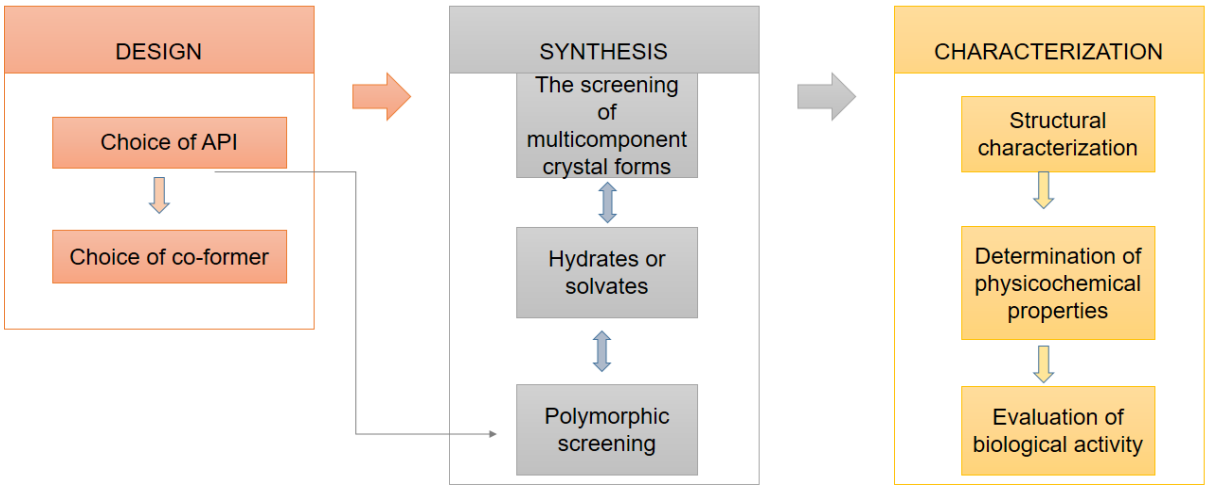

Figure 1-4 Schematic representation of the design of co-crystal of active pharmaceutical ingredients[10]

The first step is to design. At this stage, it is necessary to specify the functional groups that exist in the API of interest and, subsequently, make a survey[25, 26] in Cambridge Structural Database[9] (CSD) for most probable supramolecular synthons between the potential co-former and API of interest.[5]

The second step is the synthesis of the multicomponent form. Generally, polymorphic screening is the first stage of the synthesis in order to reveal probable solvate, hydrate and polymorphic forms of interest of API. Afterwards, the supramolecular synthesis is done with the use of suitable synthetic techniques. The mostly applied synthesis strategies are reaction crystallization method, crystallization by conventional evaporation method and mechanochemistry.

The last step is the characterization of the multicomponent solid forms, which requires powder and single-crystal X-ray diffraction (PXRD and SCXRD, respectively), solid-state Nuclear Magnetic

Resonance, FTIR, FT-Raman, thermogravimetric analysis (TGA), and Differential Scanning Calorimetry (DSC).[10]

1.4.3 Synthesis methods performed in the synthesis of co-crystals

The formation of co-crystals majorly depends on the nature of the reactants and the solvent. The success is never a guarantee since the control over nucleation, crystallization and phase evolution is an issue for co-crystal's formation. Additionally, the understanding of the formation is mostly unknown. Despite these drawbacks, there are various co-crystal preparation methods already known in the literature such as solid state grinding, solvent evaporation, solution crystallization, slurry conversion, melt crystallization, spray crystallization, and hot melt extrusion. In general, these synthetic methods can be divided into two categories: solid-state and solution based methods.[27] Within this chapter, solid-state grinding, solvent evaporation, and the slurry conversion is explained in detail.

1.4.3.1 Solution-based methods

Evaporative co-crystallization: Evaporative co-crystallization is the most conventional technique when it comes to grow single crystals suitable for SXRD measurements. The principle of this method relies on the supersaturation of the solution via evaporation, which leads to the nucleation and growth of crystals from solution. Usually, slow evaporation yields larger crystals, what is preferred. For evaporative co-crystallization, the concentration of both API and co-former have to be taken into account. In order to enlighten and guide the co-crystallization process, a few methods such as co-crystal operating range, and the analysis of ternary phase diagrams have been proposed. In spite of extra need of solvent, this technique is still the most used for industrial up-scaling processes.[27]

Slurry conversion: Slurry conversion is a method in which a fixed ratio of API and co-former is put into a suspension and stirred for some hours/days. This method requires the use of excess solid fraction over solvent. The key factors of slurry conversion are solubility, the relative concentration of the compound and the co-former. Karimi-Jafari *et al*. stated that the transformation of co-crystal is inversely proportional to the solubility behaviour of the compounds in a specific solvent[27]. Moreover, it was also shown that the use of ternary phase diagrams can be helpful and it can be used as a guideline to optimize the reaction conditions.[28]

1.4.3.2 Solid-state methods

Mechanochemistry is broadly applied in the synthesis of new co-crystals because it offers a green alternative over conventional techniques, providing simultaneously enhanced yields.

Neat (dry) grinding: As the name implies, neat grinding involves the use of both reagents in their dry form without the use of any solvent. Either using a mortar and pestle or an automated ball mill, the reagents are exposed to mechanical energy, which induces the formation of co-crystals.

Liquid-assistant grinding: Even though the principles of both grinding and liquid-assistant grinding are similar, for the application of liquid-assistant grinding, a catalytic amount of solvent is required and it can greatly facilitate the formation of co-crystals. Yet, the mechanism of how the co-crystal formation is induced with this technique is far from been fully understood.[27, 29]

1.5 Sparfloxacin

1.5.1 Sparfloxacin as Antibiotic

Sparfloxacin (SPX) is a broad-spectrum antimicrobial agent from the class of fluoroquinolone antibiotics, which was patented 1989 and launched as a medicine in 1935 for the treatment of *streptococci* and community-acquired lower respiratory tract infections.[30]

As the other quinolones, the antimicrobial activity of SPX is caused by inhibition of topoisomerase II (DNA gyrase) and topoisomerase IV, which are enzymes contributing to bacterial DNA transcription, and replication.[31, 32] It possesses in vitro activity against a wide range of gram-negative and gram-positive microorganisms.[33] Compared with its counterparts in the class of fluoroquinolone antibiotics, SPX displays enhanced microbial activity against gram-positive pathogens and better in vitro activity, especially against gram-positive *cocci* and anaerobe microorganisms.[34, 35] Whilst most of adverse effects are similar to other fluoroquinolones, SPX has a higher potential in phototoxicity,[36, 37] for that reason, in 2001, the medicine was withdrawn from the market.[38]

1.5.2 Sparfloxacin from a chemistry point of view

From the chemistry point of view, SPX is an amphoteric drug. Its empirical formula is $C_{19}H_{22}F_2N_4O_3$ and it has the following chemical structure:

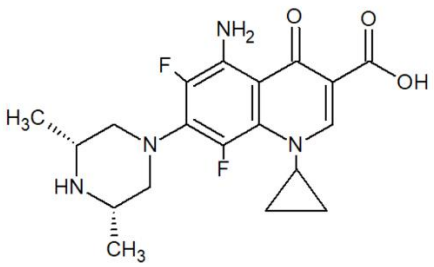

Figure 1-5 Structure of Sparfloxacin

Owing to its chemical structure, SPX has both a Bronsted acid (via oxoacid) and a Bronsted base (via organic amino compound) active sites. Furthermore, it is sparingly soluble in aqueous solution (0.113 mg/mL). Yet, SPX is not stable in the presence of water and immediately transforms into a hydrated form. Additionally, it can exist in both neutral and zwitterionic form. Control over these forms is highly important since they offer different properties. In general, amphoteric drugs offer a trade-off between high membrane permeability and high solubility. When the drug is available in neutral form, it has higher membrane permeability but suffers from lower solubility. On the contrary, zwitterionic forms of the drug generally tend to have higher solubility trend but poor membrane permeability, which results in limited bioavailability.

In CSD[9], it is possible to find the crystal structure of neutral SPX, as well as two different hydrate forms.[39-41] The refcodes of these forms are JEKMOB, COQWOU, and COQWOU01, respectively. The drug commercialized under the name of Zagam was based on SPX trihydrated form.[30]

1.5.3 Literature of Sparfloxacin multicomponent crystal forms

Even though there are many studies of SPX published in CSD[9] database, e.g. salt of SPX with tetrafluoroborate[42] or ionic metal complexes with zinc,[43] copper,[44] there is very limited co-crystal research. Gunnam et al. showed the possible co-crystal formation between SPX and methyl, ethyl, isobutyl paraben via amino phenol synthon recognition.[45] To the best of our knowledge, there are no other studies reporting the formation of SPX multicomponent crystal forms.

1.6 Work outline and objective

With this work it is aimed to expand the pharmaceutical solid-state forms of SPX to alter its physicochemical properties. Furthermore, it is also intended to stabilize the zwitterionic characteristic of SPX, which majorly limits its bioavailability. For this reason, anthranilic acid, 3-aminobenzoic acid, 4-aminosalicylic acid and nalidixic acid were chosen as co-formers. The structures of GRAS co-formers are shown in Figure 1-6.

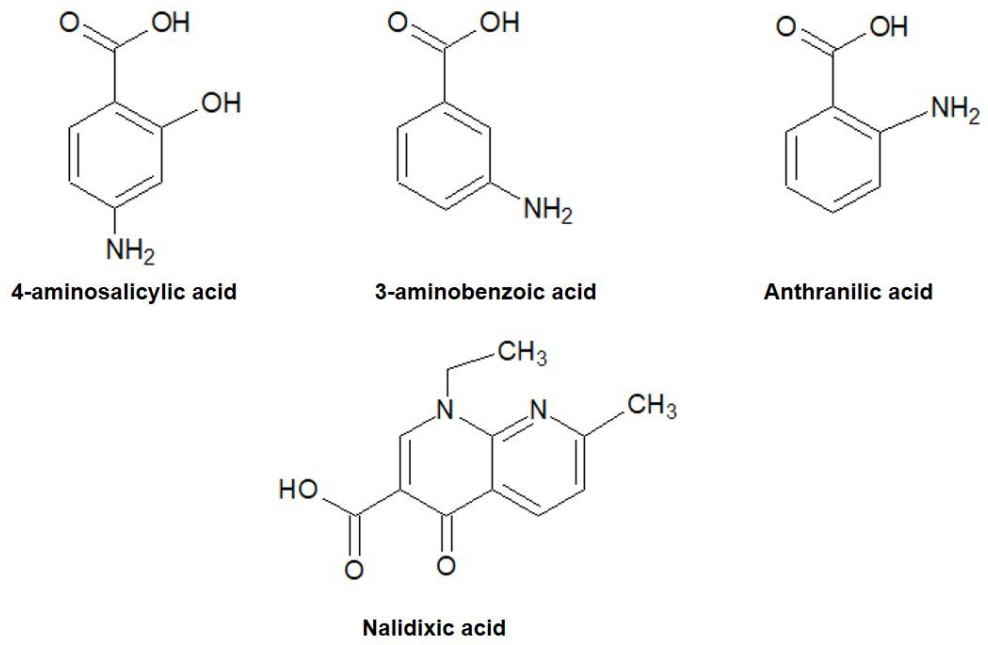

Figure 1-6 The structure of GRAS co-formers performed in this study

In this study, the co-formers possess –COOH and –NH_2 moieties, as these moieties are capable of providing hydrogen bond interactions with SPX. Important to note here is that the co-formers used have the –COOH and –NH_2 groups in different positions.

Table 1-1 The summary of pka values of SPX and the co-formers

Compound and co-former	**pKb of SPX**[30]	**pKa of coformer**[46-48]	**ΔpKb-a**
SPX +4 ASA	8.79	3.68	5.11
SPX + 3ABA	8.79	4.81	3.98
SPX + AA	8.79	4.89	3.98
SPX + NA	8.79	5.89	2.90

The multicomponent crystal forms between SPX and 4-ASA have a special interest as they are both antibiotics and therefore the newly obtained molecular salts can possibly has superior biological activity

In this regard, the first chapter of this dissertation is dedicated to the introduction that explains briefly the fundamental concepts of co-crystal formation e.g. crystal engineering, supramolecular synthon

theory, and graph-set analysis, the steps of co-crystal design, synthetic methods.

The second chapter investigates the polymorphic and solvate screening of SPX. This chapter is a fore-step of co-crystal screening. Within this chapter, the probable solvate and polymorphic forms are enclosed.

The third chapter is dedicated to the co-crystal screening of SPX. Co-crystal forms of SPX with previously mentioned GRAS co-formers are investigated, as well as the changes they induce in the physicochemical properties of the API, e.g. solubility, and stability.

At the end of the second and the third chapters, conclusion and future perspective can be found. Within conclusion and future perspective, the most significant aspects of the research and results are mentioned. Moreover, the issues have been encountered throughout the study and possible alternative solutions are also discussed.

Chapter 2

Polymorphic Screening of Sparfloxacin

2.1 Introduction

Throughout the downstream process of the majority of API manufacturing, crystallization is applied as a purification method and this stage may induce organic solids to crystallize into multiple forms. Control over the multiple forms of APIs is crucial for the consistent product quality. There are many examples highlighting the importance of polymorphic screening. For example, it has been shown that solubility can be raised four times by using a different polymorphic form of risperidone.[49] Also the the oral bioavailability of the product as well as the physical stability of the drug depend on which porlymorph of the API is being used. Hence, it is essentiall to investigate for possible polymorphic forms of the API as well as solvate and hydrate forms.

A new form of SPX, either solvate or polymorph, was encountered throughout the reaction attempts of co-crystal formation between Nalidixic acid and SPX using ACN and EtOH as solvents in the previous work done by other members of our research group. Therefore, these experimental conditions were also used in this polymorphic study to futher investigation of the form.

2.2 Materials and Methods

2.2.1 Materials

All the reagents and solvents were purchased from Sigma-Aldrich, Fluka, Sigma, Aldrich and Alfa Aeser and used without further purification.

2.2.2 Methods

Powder X-ray diffraction (PXRD): Samples were analysed by X-ray powder diffraction, using two diffractometers:

1- D8 Advance Bruker AXS θ-2Θ diffractometer, with a copper radiation source (Cu Kα, λ= 1.5406 Å) and a SSD160 detector, operating at 40 kV and 30 mA. Throughout the measurements, Ni filter was used in the data collections
2- D8Advance Bruker diffractometer, with a copper radiation source (Cu Kα, λ= 1.5406 Å) and a Linxeye-XE detector, operating at 40 kV and 30 mA. Throughout the measurements, no Ni filter was used in the data collections, relying in the capability of the detector to minimize Kβ.

Single crystal X-ray diffraction (SCXRD): Suitable crystals of the acetonitrile solvate were selected

and mounted on a loop with Fomblin protective oil. Data was collected on a Bruker AXS-KAPPA APEX II diffractometer at 150 K and using a Bruker AXS-KAPPA D8 - QUEST at 293 K, with graphite-monochromated radiation (Mo K α, λ= 0.71073 Å). The X-ray generator was operated at 50 kV and 30 mA, and the X-ray data collection was monitored by the APEX3 program.

Details on the SCXRD details are given in Table 2-1.

Table 2-1 Crystallographic details of ACN solvate of Sparfloxacin

Structure	**SPX ACN solvate**
Empirical formula	$C_{20}H_{23.50}F_2N_{4.50}O_3$
Formula weight	412.93 g/mol
Crystal system, Space group	Orthorhombic, *Pcca*
Unit cell dimensions	a = 30.867 (4) Å, α = 90º b = 9.4078(13) Å, β = 90º c = 13.908(2) Å, γ = 90º
Absorption coefficient	0.106 mm^{-1}
F (000)	1736
Temperature	293 (2) K
Wavelength	0.71073 Å
Volume	4038.9 $Å^3$
Z, calculated density	8.1358 mg/cm^3
Crystal size	0.008 x 0.004 x 0.002 mm
Theta range	2.639-26.444º
Limiting indices	-38<=h<38, -11<=k<11, -17<=l<17
Refinement method	Full-matrix least-squares on F^2
Reflections collected/unique	99735/4125 [R(int)=0.1654]
Data/ restraints parameters	4125 /3 /288
Completeness	99.3%
Goodness-of-fit on F^2	1.146
Final R indices [I>2σ(I)]	R_1 = 0.0980, wR_2 = 0.1817
R indices(all data)	R_1 = 0.1692, wR_2 = 0.2115
Large diff. peak and hole	0.390 e $Å^{-3}$
Extinction coefficient	n/a

Differential Scanning Calorimetry (DSC) and Thermogravimetric Analysis (TGA): Both DSC and TGA were performed using a SETARAM TG-DTA 92 thermobalance under nitrogen flow with a heating rate of 10°C.min-1 for the acetonitrile solvate (5-10 mg).

2.3 Synthesis

SPX-DMSO-S, Sparfloxacin in DMSO: 50 mg of SPX (0.127 mmol) was dissolved with 5 ml of DMSO at 120 °C and then, the solution was left for slow evaporation.

SPX-DMSO-Slu, Sparfloxacin in DMSO: 50 mg of SPX (0.127 mmol) was placed into a vial and subsequently 1 ml of DMSO solution was added. Afterwards, the solution was left stirring for 27 hours.

SPX-NA-S-ACN:EtOH, Sparfloxacin and Nalidixic acid in ACN:EtOH: The mixture of 0.06282 g of SPX (0.160 mmol) and 0.03717 g of NA (1:1 molar ratio) was dissolved in 6 ml of a 1:1 mixture of ACN:EtOH upon heating to 65ºC. The pH of the reaction medium was 5.5. At the end, the solution was left to crystallize for slow evaporation of the solvent at room temperature.

SPX-S-ACN:EtOH, Sparfloxacin in ACN:EtOH: 0.06282 g of SPX (0.160 mmol) was dissolved in 7 ml of solvent mixture of ACN:EtOH (1:1) upon heating to 65℃ . Subsequently, the pH of the reaction medium was 6 and the solution was left crystallize by slow evaporation of the solvent at room temperature. Yet the solution did not yield any single crystals, and powder was obtained.

SPX-NA-Slu-ACN:EtOH, Sparfloxacin and Nalidixic acid in ACN:EtOH: 0.06282 g of SPX (0.160 mmol) and 0.03717 g of NA (1:1 molar ratio) were stirred in 2 ml of a ACN:EtOH mixture at room temperatrue for 27 hours. The solution was then left to evaporate.

SPX-Slu-ACN:EtOH, Sparfloxacin in ACN:EtOH: 0.06282 g of SPX (0.160 mmol) were stirred in 2 ml of a ACN:EtOH mixture at room temperatrue for 27 hours. The solution then was left to evaporate.

SPX-NA(4:1)-S-ACN:EtOH, Sparfloxacin and Nalidixic acid in ACN:EtOH: The mixture of 0.0357 g of SPX (0.090 mmol) and 0.003537 g of NA (0.0225), was dissolved in 10 ml of ACN:EtOH (1:1) upon heating to 65℃. At the end, the solution was left to crystallize for slow evaporation of the solvent at room temperature. Yet the solution did not yield any single crystals, and powder was obtained. .

SPX-ACN-Slu-48h, Sparfloxacin in ACN: 50 mg of SPX (0.127 mmol) was placed into a vial and subsequently 1 ml of ACN solution was added. Afterwards, the solution was left for stirring for 48 hours.

SPX-EtOH-Slu-48h, Sparfloxacin in EtOH: 50 mg of SPX (0.127 mmol) was placed into a vial and subsequently 1 ml of EtOH solution was added. Afterwards, the solution was left for stirring for 48 hours.

2.4 Results and Discussion

In order to follow the experimental progress, all the experimental attempts were firstly characterized by PXRD measurements. Afterwards, depending on the successful results obtained by PXRD, experimental characterization was taken to the further stages.

Table 2-2 The polymorphic screening conditions of Sparfloxacin

Solvent	New Form	Crystal Structure
DMSO	Yes	No
EtOH	Yes	No
ACN	No	No
ACN:EtOH (1:1)	No	No
Nalidixic acid ACN:EtOH (1:1)	Yes	Yes

DMSO solvate

The results of **SPX-DMSO-S** and **SPX-DMSO-Slu** experimental procedures were analysed with PXRD measurements. The comparison of experimental result and simulated SPX patterns from CSD[9] database can be found in Figure 2-1.

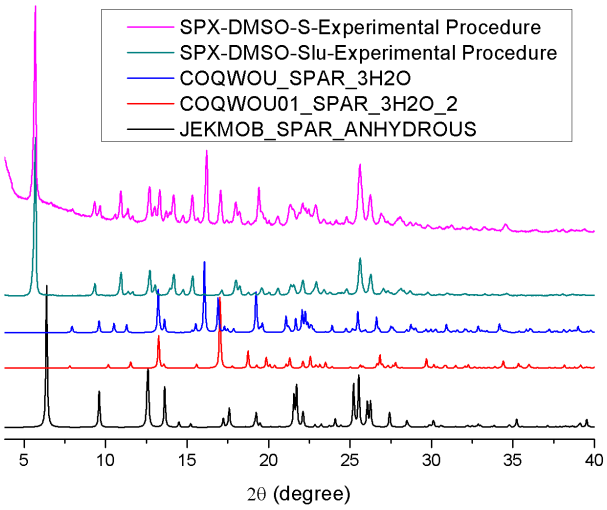

Figure 2-1 The comparison of PXRD patterns of SPX-DMSO-S and SPX-DMSO-Slu experimental procedures with Sparfloxacin with the crystal forms deposited at CSD.

According to the PXRD results, it is possible to say that both experimental PXRD results are different from the simulated SPX patterns, which indicates either the formation of a solvate or a new polymorph. Comparing both experimental patterns, even though they look mostly identical, the result of evaporative crystallization procedure has extra peaks over the slurry conversion experimental procedure. This might

indicate that the evaporative crystallization procedure contains the same form obtained by slurry with some impurities. Unfortunately, due to the unsuccessful attempts of obtaining single crystals of these new forms, their structural characterization is still an on-going process.

ACN and EtOH solvates

Apart from the use of DMSO as solvent, our interest was shifted towards more volatile, easy to use solvents such as ACN and EtOH. As it was previously mentioned, there is a new form obtained by the use of Sparfloxacin, Nalidixic acid with the use of ACN and EtOH (1:1) solvent system. This new form corresponds to an acetonitrile solvate of SPX, as proved by the SXRD results (Figure 2-2), and therefore it is possible to obtained a theoretical powder diffraction pattern.

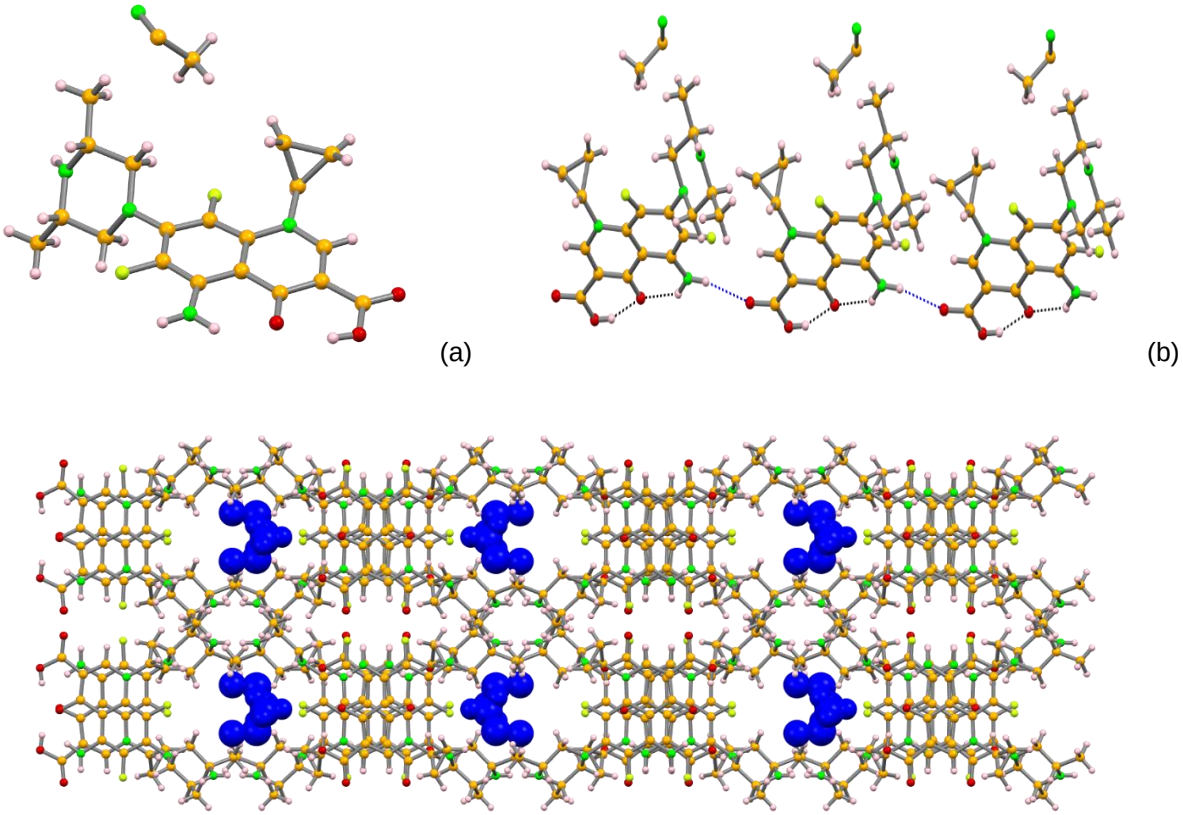

Figure 2-2 Illustration of ACN solvate crystal structure depicting: (a) the assymetric unit; (b) the intramolecular (black) and intermolecular (blue) hydrogen bonds established; and (c) the supramolecular arrangengement in a view along the c axis

The asymmetric unit of the ACN's solvate consists (Figure 2-2.(a)) of one molecule of SPX and an acetonitrile molecule, with the ACN molecule residing on a special position, with half occupation factors. Both intramolecular hydrogen bonds established between the N-H_{NH2} and the carbonyl and the O-H_{COOH} and the carbonyl are maintained in the new solvate. Also the type of interactions between consecutive SPX molecules (N-H_{NH2} ⋯ O-H_{COOH}) is similar to the interactions observed in SPX alone (Figure 2-2

(b)). Hydrogen bond details are given in Table 2-3.

Regarding the global supramolecular arrangement of this form, it is particularly interesting that, in a view along *c* (Figure 2-2.(c)), the ACN molecules lie in porous formed by the packing of SPX molecules.

Table 2-3 Hydrogen bonding details of ACN solvate of Sparfloxacin

Structure	**(D)-H…A**	**Symmetry operator**	**D…A /Å**	**D…H /Å**	**H…A/ Å**	**D-H…A /º**
SPX ACN solvate	N_1-H_1…0_3	x,y,z	2.645 (5)	0.90 (7)	1.9 (8)	138 (6)
	O_2-H_2…0_3	x,y,z	2.530 (5)	0.82	1.77	153
	N_2-H_2…F_2	x,y,z	2.670 (5)	0.886 (16)	2.35 (3)	101 (2)
	N_2-H_2…O_1	x, -1+y, z	3.118 (5)	0.8886 (16)	2.292 (18)	155 (2)
	C_{10}-H_{10}…F_2	x, 1+y, z	3.352 (5)	0.93	2.46	162
	C_{10}-H_{10}…0_1	x,y,z	2.778 (6)	0.93	2.45	101
	C_{17}-H_{17}…F_1	x,y,z	2.723 (6)	0.97	2.21	112

However, this solvate was never obtained as a pure phase and, in the light of this, it was attempted to further explore options to obtain this form as a pure phase. Therefore, the reaction conditions were mimicked with and without the use of nalidixic acid for the further investigation of the new form. The obtained PXRD results are illustrated in Figure 2-3.

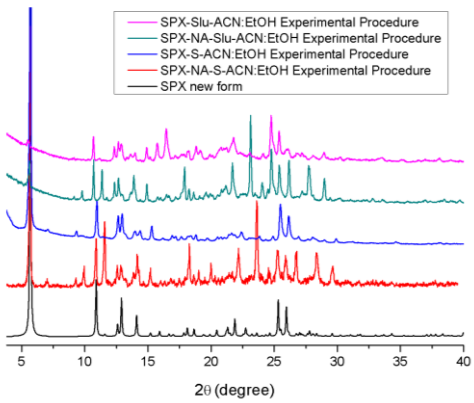

Figure 2-3 Comparison of the PXRD results of the related experimental synthesis with the simulated solvate form

As it can be observed from PXRD patterns, none of the experimental conditions resulted in the pure new form. Even though there are common peaks and quite repetative in almost all the synthesis conditions, there are also extra phases in all the experimental diffractograms (Figure 2-3). In this sense, it can be concluded that formation of this form might be somehow stabilized or induced in the presence of nalidixic acid with the application of the solvent system mentioned above. The reason is that the PXRD pattern of experimental procedure including nalidixic acid is the closest one to the new form.

Subsequently, it was hypothezsized that the use of catalytic amount of NA could be effective for the formation of this form. Hence, the reaction conditions in which the 1:1 molar ratio were changed into 4:1 (SPX:NA). The PXRD result of 4:1 molar ratio of SPX to NA is illustrated in Figure 2-4.

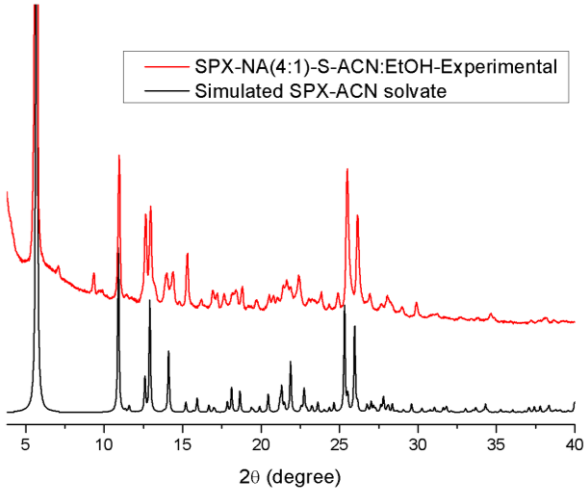

Figure 2-4 Comparison of PXRD result of SPX-NA(4:1)-S-ACN-EtOH experimental procedure with the simulated solvate form

On the basis of the comparison of the experimental and theoretical PXRD patterns, it can be mentioned that the use of less amount of NA reduced the extra phases which was obtained on previous experimental results. This result indicates that the amount of NA is highly important. However, the experimental PXRD still includes extra phase(s), which can be attributed to anhydrous SPX (Figure 2-4).

Further experiments were carried out to try to obtain the pure ACN solvate, (**SPX-ACN-Slu- 48h** and **SPX-EtOH-Slu-48h**), was perfomed in order to observe indivual possible solvate formation. Here in with this attempt, it was aimed to enlarge the reaction time to provide enough of time for the transformation of the new form. The Figure 2-5 shows the PXRD results of **SPX-ACN-Slu- 48h** and **SPX-EtOH-Slu-48h** experimental procedures compared with new form.

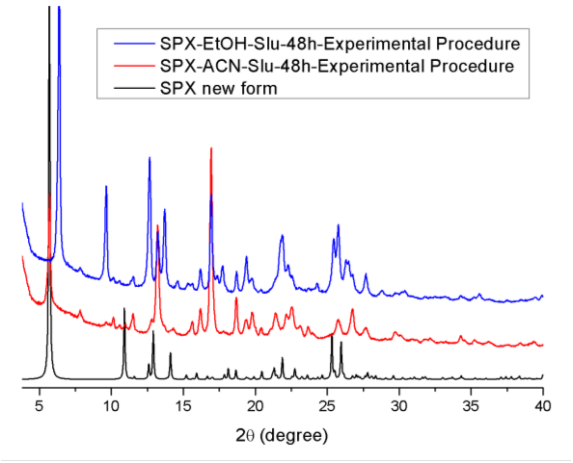

Figure 2-5 Comparison of PXRD results of SPX-EtOH-Slu-48h and SPX-ACN-Slu-48h experimental procedures with the new form

Based on the PXRD results, it can be mentioned that slurries both solvents resulted in a different PXRD patttern than the ACN solvate (Figure 2-5). In these conditions, it can be stated that NA plays an important role in the formation of this form and this form was not succesfully obtained without the use of nalidixic acid under this reaction conditions.

Additionally, the results of **SPX-EtOH-Slu-48h** and **SPX-ACN-Slu-48h** are also compared with simulated SPX forms available in CSD[39, 41]. The related PXRD patterns are shown in Figure 2-6.

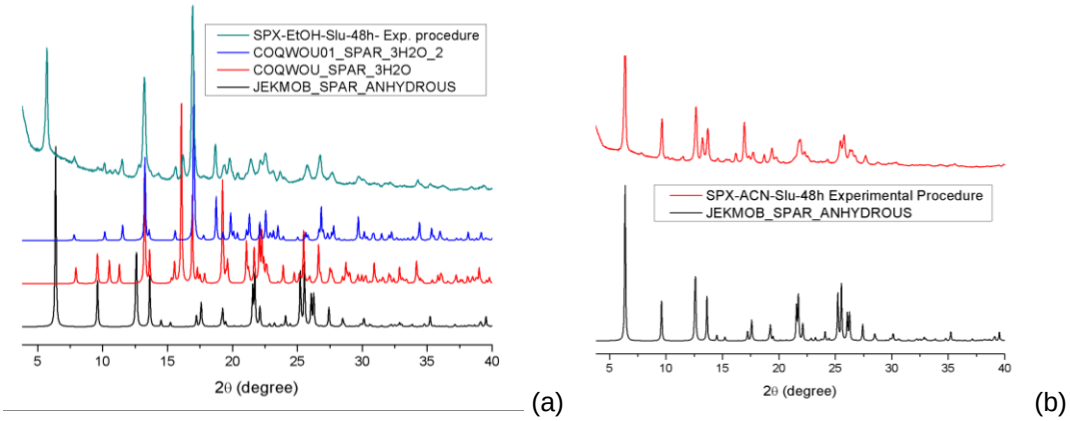

Figure 2-6 Comparison of PXRD patterns of simulated SPX patterns with (a) SPX-EtOH-Slu-48h (b) SPX-ACN-Slu-48h

The comparison of PXRD patterns indicates that a new form is obtained by **SPX-EtOH-Slu-48h** experimental procedure since the pattern is not identical to other simulated patterns of SPX (Figure 2-6 (a)). In this regard, it can be stated that there is a new form of SPX, which can be obtained using EtOH (Figure 2-6). Despite on the efforts made to obtain single crystals for further structural analysis no successfull attempt was yet possible. Hence, this form remains as an on-going study subject.

On the other hand, there was no change in the PXRD pattern of **SPX-ACN-Slu-48h** experimental procedure, (Figure 2-6 (b)), indicating that neither a solvate nor a new polymorph are obtained.

Even though it was not possible to obtain a pure phase of the ACN solvate, TGA-DSC measurements were carried out for the **SPX-NA(4:1)-S-ACN:EtOH** procedure to further demonstrate the presence of ACN. The results of TGA-DSC can be found in Figure 2-7.

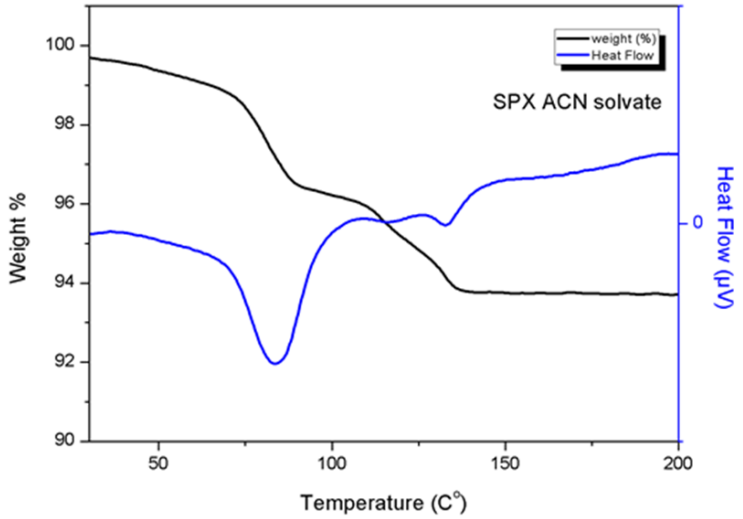

Figure 2-7 The TGA-DSC result of the ACN solvate

Two phenomena are detected before 200°C in the TGA/DSC data (Figure 2-7) corresponding to endothermic events with mass loss associated. The first event occurs at around 88ºC with approximately 4.5% of mass reduction whereas the second one occurs around 136ºC with approximately 2.58 % of mass reduction. According to the calculations based on the molecular weight of the ACN:solvate, the loss of ACN corresponds to 2.52 %, value that is in agreement with the second event detected. The first endothermic peak in de DSC and the corresponding mass loss are most likely related with the other form (most likely a hydrated form) present in the bulk sample that was analysed.

2.5 Conclusion and Future Perspective

Throughout this chapter, the investigation of polymorphic forms of SPX as well as solvate forms was investigated. Based on the results mentioned before, it can be said that there are three different forms of SPX encountered within this study. The use of DMSO, EtOH, and ACN:EtOH with NA led to the formation of those new forms. However, the full study of none of these forms is totally concluded yet.

The nature of the solvent creates the biggest problem with the crystallization for the form that was obtained with DMSO because this solvent is not volatile; hence, it is hard to grow single crystals. However, one approach could be the recrystallization of the product instead of application of slow

evaporation method. Yet again recrystallization requires many attempts and time. Also other crystallization methods, such as the use of anti-solvents, can be an alternative method for the production of these crystals.

On the other hand, the use of EtOH does not properly dissolve the SPX compounds, therefore, there was never a clear solution obtained for crystallization. One approach could be the use of the product and then the recrystallization of the crystal. In addition to that, anti-solvents could also be an alternative again.

Lastly, the acquiring of the ACN solvate of SPX was attempted to be obtained as a pure form though the result was unfortunately not satisfactory. In order to obtain this form as a pure phase, the use of reaction crystallization instead of slow evaporation might be an alternative approach. Asides from experimental methods, the reaction conditions such as time, and concentration could also be critical factors. Therefore, there is a need for a more detailed and systematic approach.

Bringing all together, there might be other polymorphic and solvate forms of SPX, which can possibly alter the properties of the API. However, the investigation of these forms requires further research, time and effort, as well as the application of alternative experimental methods and conditions.

Chapter 3

Screening of Co-crystals and Salts of Sparfloxacin

3.1 Introduction

In general, co-crystal and salt screening is applied in the development stage of APIs in order to bring a solution of a problem that can be related with solid form or formulation. In addition to that, co-crystal and salt screening can also be performed in order to target solubility, dissolution rate, and bioavailability issues. In this regard, co-crystal and salt transformation can be carried out for zwitterionic compounds such as SPX to overcome the trade-off between high solubility and low membrane permeability of the API. This approach has already been proposed for other quinolones as a way of improving both solubility and membrane permeability[45]. With this sense, we decided to investigate the possibility of extending the possibilities of multicomponent crystal forms of SPX.

3.2 Materials and Methods

3.2.1 Materials

All the reagents and solvents were purchased from Sigma-Aldrich, Fluka, Sigma, Aldrich and Alfa Aeser and used without further purification.

3.2.2 Methods

Powder x-ray diffraction (PXRD): Samples were analysed by X-ray powder diffraction, using two diffractometers:

1- D8 Advance Bruker AXS θ-2Θ diffractometer, with a copper radiation source (Cu Kα, λ= 1.5406 Å) and a SSD160 detector, operating at 40 kV and 30 mA. Throughout the measurements, Ni filter was used in the data collections
2- D8Advance Bruker diffractometer, with a copper radiation source (Cu Kα, λ= 1.5406 Å) and a Linxeye-XE detector, operating at 40 kV and 30 mA. Throughout the measurements, no Ni filter was used in the data collections, relying in the capability of the detector to minimize Kβ.

Single crystal x-ray diffraction (SCXRD): Suitable crystals of each salt were selected and mounted on a loop with Fomblin protective oil. Data were collected on a Bruker AXS-KAPPA APEX II and a Bruker AXS-KAPPA D8 - QUEST diffractometers at 293 K, with graphite-monochromated radiation (Mo K α, λ= 0.71073 Å). The X-ray generators were operated at 50 kV and 30 mA, and the X-ray data collection was monitored by the APEX2 and APEX3 program.

Table 3-1 Crystallographic details of multicomponent forms of Sparfloxacin

Structure	SPX:4-ASA Form I	SPX:4-ASA Form II	SPX-AA
Empirical formula	$C_{26}H_{36}F_2N_5O_{14}$	$C_{13}H_{14}FN_{2.50}O_3$	$C_{26}H_{28}F_2N_5O_6$
Formula weight	680.60 g/mol	272.77 g/mol	529.54 g/mol
Temperature	293(2) K	296(2) K	293 (2) K
Wavelength	0.71073 Å	0.71073 Å	0.71073 Å
Limiting indices	-17<=h<=17, -39<=k<=39, -8<=l<=8	-23<=h<=23, -8<=k<=8, -26<=l<=25	-23<=h<=23, -8<=k<=8, -26<=l<=25
Refinement method	Full-matrix least-squares on F^2	Full-matrix least-squares on F^2	Full-matrix least-squares on F^2
Crystal system	Monoclinic	Monoclinic	Orthorhombic
Space group	*P* $2_1/c$	*P* $2_1/n$	*Pbca*
Unit cell dimensions	a = 14.259(3) Å, b = 32.437(5) Å, c=7.1362(13) Å, α = 90º β = 98.72(5)º γ = 90º	a = 18.5866(12) Å, b = 7.1168(5) Å, c = 21.1074(13) Å, α = 90º β = 94.127(3)º γ = 90º	a = 7.555 (11) Å, b = 15.502 (2) Å, c = 41.46 (6) Å, α = 90º β = 94.127(3)º γ = 90º
Volume	3262.4(10) $Å^3$	2784.8(3) $Å^3$	4856(13) $Å^3$
Z, calculated density	4, 1.386 mg/m^3	8, 1.301 mg/m^3	8, 1.449 mg/m^3
Reflections collected/unique	41239 / 6295 [R(int) = 0.1413]	36119 / 5709 [R(int) = 0.0674]	100518 / 5026 [R(int) = 0.2272]
Data/ restraints/ parameters	6295 / 8 / 484	5709 / 6 / 378	5026 / 4 / 359
Absorption coefficient	0.120 mm^{-1}	0.102 mm^{-1}	0.112 mm^{-1}
F (000)	1428	1144	2224
Crystal size	0.14 x 0.08 x 0.04 mm	0.18 x 0.10 x 0.04 mm	0.40 x 0.06 x 0.02 mm
Theta range	2.374 to 25.903º	1.410 to 26.535º	2.628 to 26.511º
Completeness	99.9%	99.5%	100.0 %
Final R indices [I>2sigma(I)]	R1 = 0.1248, wR2 = 0.3449	R1 = 0.0693, wR2 = 0.2088	R1 = 0.1328, wR2 = 0.2217
R indices (all data)	R1 = 0.2105, wR2 = 0.4133	R1 = 0.1225, wR2 = 0.2532	R1 = 0.2501, wR2 = 0.2673
Goodness-of-fit on F^2	1.362	1.003	1.110
Large diff. peak and hole	1.691 and -0.792 e $Å^{-3}$	0.595 and -0.306 e $Å^{-3}$	0.588 and -0.363 e $Å^{-3}$
Excinction coefficient	n/a	n/a	n/a

Forms	SPX:3-ABA Form I	SPX:3-ABA Form II
Empirical formula	$C_{34.67}H_{41.33}F_{2.67}N_{6.67}O_8$	$C_{52}H_{58}F_4N_{10}O_{12}$
Formula weight	730.07 g/mol	1091.08 g/mol
Temperature	293 (2) K	296(2) K
Wavelength	0.71073 Å	0.71073 Å
Limiting indices	-52<=h<52, -9<=k<9, -19<=l<19	-9<=h<9, -13<=k<13, -20<=l<20
Refinement method	Full-matrix least-square on F^2	Full-matrix least-square on F^2
Crystal system, Space group	Orthorhombic *Pbca*	Triclinic *P-1*
Unit cell dimensions	a=42.168 (5) Å b=7.7573(10) Å c=15,6185(19) Å α = 90º β = 90º γ=90º	a=7.8693(10) Å b=10.6826(13) Å c=16,372(2) Å α = 90º β = 90º γ=90º
Volume	5109.0(11)$Å^3$	1341.0(3) $Å^3$
Z, calculated density	6.1424 mg/m^3	1.1351 mg/m^3
Reflections collected/unique	32024/ 5211 [R(int)=0.0924]	13493 / 5368 [R(int)]
Data/ restraints parameters	5211 / 0 / 386	5368 / 6 / 386
Absorption coefficient	0.112 mm^{-1}	0.106mm^{-1}
F (000)	2304	572
Crystal size	0.200 x 0.060 x 0.040 mm	0.200 x 0.800 x 0.050 mm
Theta range	2.608-26.380º	2.915 to 26.420º
Completeness	99.8 %	98.0 %
Goodness-of-fit on F^2	1.099	1.014
Large diff. peak and hole	0.190 and -0.231e $Å^{-3}$	0.563 and -0.194 e $Å^{-3}$
Extinction coefficient	n/a	n/a

Fourier Transform Infrared Spectroscopy (FT-IR): FT-IR analysis was performed by using Nexus-Thermo Nicolet spectrometer (64 scans and resolution of 4 cm^{-1}) in the 4000−400 cm^{-1} range. Samples were prepared in KBr (1:100 in weight).

Differential Scanning Calorimetry (DSC) and Thermogravimetric Analysis (TGA): Both DSC and TGA was performed by using SETARAM TG-DTA 92 thermobalance under nitrogen flow with a heating rate of 10°C.min^{-1} for the sample (5-10 mg).

Preliminary/Empirical Solubility Studies: 10 mg of each new multicomponent form were added to 10 ml of H_2O and stirred; as control, 10 mg of SPX were also added to 10 ml of water and stirred. The comparison between the clarity of the final solutions was used to estimate the relative solubility behaviour.

3.3 Synthesis of multicomponent forms of Sparfloxacin with 4-Aminosalicyclic acid, 3-Aminobenzoic acid, Anthranilic acid and, Nalidixic acid

3.3.1 Synthesis of Sparfloxacin and 4- Aminosalicyclic acid salts

SPX-4ASA-M-DMF, Sparfloxacin and 4-aminosalicylic acid salt: SPX (0.0357 g) and 4-ASA (0, 0142 g), corresponding to 1:1 molar ratio, were manually grinded in a mortar with the addition of 200 μl of dimethylformamide (DMF) for 15 minute.

SPX-4ASA-S-EtOH:H_2O, Sparfloxacin and 4-aminosalicylic acid salt: SPX (0.0357 g) and 4-ASA (0.0142 g), corresponding to 1:1 molar ratio, was dissolved with the addition of 20 ml (1:1) EtOH:H_2O solvent mixture at 50℃ for 10 minute. Later, the solution was left for slow evaporation. Crystals with needle shape was obtained after 3-5 days.

SPX-4ASA(1:1)-M-ACN-EtOH:H_2O, Sparfloxacin and 4-aminosalicylic acid salt: SPX (0.0539 g) and 4-ASA (0.210 g), corresponding to 1:1 molar ratio, were placed into a mortar. Subsequently, the reagents were manually grinded with the addition of 250ml EtOH:H_2O (1:1) solvent mixture for 15 min. Light yellow powder was obtained.

SPX-4ASA(2:1)-M-ACN-EtOH:H_2O, Sparfloxacin and 4-aminosalicylic acid salt,: SPX (0.0628 g) and 4-ASA (0.0122 g), corresponding to 2:1 molar ratio, were placed into a mortar, subsequently, the reagents were manually grinded with the addition of 200 μl EtOH:H_2O (1:1) solvent mixture for 15 min. Light yellow powder was obtained.

3.3.2 Synthesis of Sparfloxacin and 3-Aminobenzoic acid salts

SPX-3ABA-Slu-THF, Sparfloxacin and 3-aminobenzoic acid salt: SPX (0.0357 g) and 3-aminobenzoic acid (0.0142g), corresponding to 1:1 molar ratio, were placed into a flask and stirred for 27 hour with the addition of 1 ml of THF. Subsequently, the solution was left for drying at room temperature.

SPX-3ABA-Slu-H_2O Sparfloxacin and 3-aminobenzoic acid salt: SPX (0.0357 g) and 3-ABA (0.0142 g), corresponding to 1:1 molar ratio, was placed into a flask and stirred for 27 hour with the addition of 1 ml of H_2O. Afterwards, the solution was left for drying under room temperature.

3.3.3 Synthesis of Sparfloxacin and Anthranilic acid salt

SPX-AA-S-ACN:EtOH, Sparfloxacin and anthranilic acid salt: SPX (0.0370 g) and anthranilic acid (0.0129 g), corresponding to 1:1 molar ratio, was dissolved with 8 ml of ACN:EtOH (1:1) solvent mixture

at 80℃ for 30 minute. Then, the solution was left for slow evaporation and the formation of yellow needle crystals were observed within 3-5 days.

3.4 Synthesis of Sparfloxacin, Nalidixic acid and 4-Aminosalicylic acid multicomponent form

Sparfloxacin and Nalidixic acid and 4-aminosalicylic acid, SPX-NA-4ASA-M-ACN:EtOH: SPX (0.05756 g) and 4-ASA (0.295 g) and NA (0.0447 g), corresponding to 1:1:1 molar ratio, were placed into a mortar. Subsequently, the reagents were manually grinded with the addition of 450 μl EtOH:H2O (1:1) solvent mixture for 15 min. Light yellow powder was obtained.

3.5 Results and Discussion

3.5.1 Introduction

Within this chapter, multicomponent crystal forms of SPX were obtained using three different co-formers: 4-aminosalicyclic acid, 3-aminobenzoic acid, anthranilic acid. Multiple forms were obtained with 4-aminosalicyclic acid and 3-aminobenzoic acid, and just a single form was synthesized with anthranilic acid.

Table 3-2 Summary of the results obtained in the co-crystal and salt screening

Co-former	Synthetic procedure	Name	Stoichiometry	Co-crystal vs salt
4ASA	**SPX-4ASA-S-EtOH-H_2O**	**SPX:4ASA Form I**	1 SPX^+ : 1 $4ASA^-$: xH_2O	salt
4ASA	**SPX-4ASA-M-DMF**	**SPX:4ASA Form II**	1 SPX^+ : 1 $4ASA^-$	salt
4ASA	**SPX-4-ASA(2:1)-M-ACN:EtOH**	**SPX:4ASA Form III**	2 SPX^+ : 1 $4ASA^-$	salt
3ABA	**SPX-3ABA-Slu- H_2O**	**SPX:3ABA Form I**	1 SPX^+ : 1 $4ASA^-$: H_2O	salt
3ABA	**SPX-3ABA-Slu-THF**	**SPX:3ABA Form II**	1 SPX^+ : 1 $4ASA^-$: H_2O	salt
AA	**Spx-AA-S-ACN:EtOH**	**SPX:AA**	1 SPX^+ : 1 AA^-	salt

3.5.2 Multicomponent crystal forms screening with Sparfloxacin and 4-Aminosalicylic acid

In the literature, it is possible to find examples of crystal forms that combine two different antibiotics based on the crystal engineering approach.[50] Inspired by those works, in this study, it is aimed to combine two different antibiotics, namely Sparfloxacin and 4-ASA, with the hope of boosting the antimicrobialactivity of the newly combined drug form. The molecular structure of 4-ASA is represented in Figure 3-1.

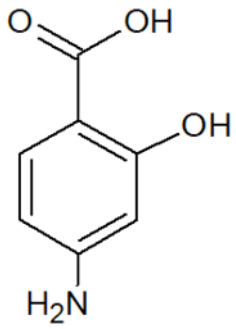

Figure 3-1 Molecular structure of 4-aminosalicylic acid

As can be seen, 4-ASA has three hydrogen bonding sites: aromatic carboxyl moiety, aromatic amine and hydroxyl groups (Figure 3-1), which are capable of contributing to the co-crystal or salt formation. Considering the active hydrogen bonding sites of SPX, it can be mentioned that there are probabilities of contact with all substituents present in 4-ASA. Similar to the theoretical expectations which offer salt formation due to pKa difference between SPX[30] and 4-ASA,[48] salt formation was observed between these two drugs in the new multicomponent forms. In this study, the refcode of 4-ASA is used as AMSALA02.

Throughout this study, there were three different salts were obtained with the use of 4-ASA as co-former. Different methods such as solution crystallization and manual grinding were applied in synthesis of these salts. The details of these multicomponent forms are mentioned below.

Structural Characterization of SPX:4ASA Form I

Subsequent to the synthesis of **SPX:4ASA Form I**, PXRD measurement was performed to assess its purity. The comparison of experimental PXRD pattern with starting reagents as well as the simulated **SPX:4ASA Form I** obtained from the crystal structure determined from SCXRD data is shown in Figure 3-2.

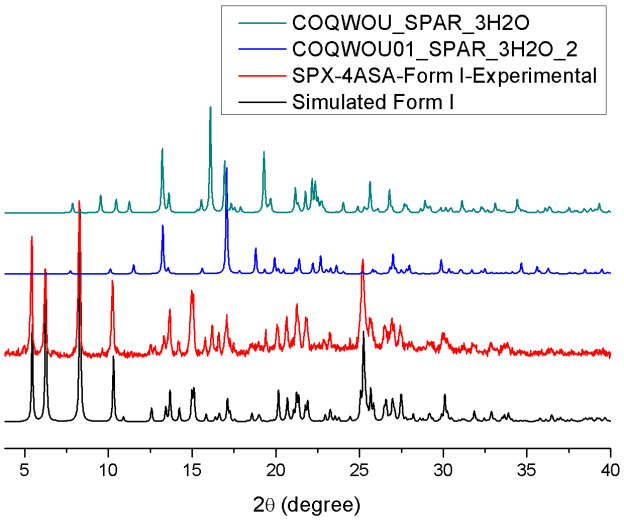

Figure 3-2 The comparison of experimental PXRD experimental pattern of Form I with starting reagents from CSD and the simulated form by SCXRD

Based on the comparison of PXRD patterns, the formation of the new form can be stated since the experimental diffractogram is not the representative of starting reagents. Furthermore, experimental PXRD pattern is identical to the simulated **SPX:4ASA Form I**, which proves the formation of pure phase multicomponent form (Figure 3-2).

For further structural information, the result of SCXRD result, which was previously investigated within the group,[51] is discussed below. The illustration of the asymmetric unit, the intermolecular and intramolecular interaction as well as the crystal packing of **SPX:4ASA Form I** is shown in Figure 3-3.

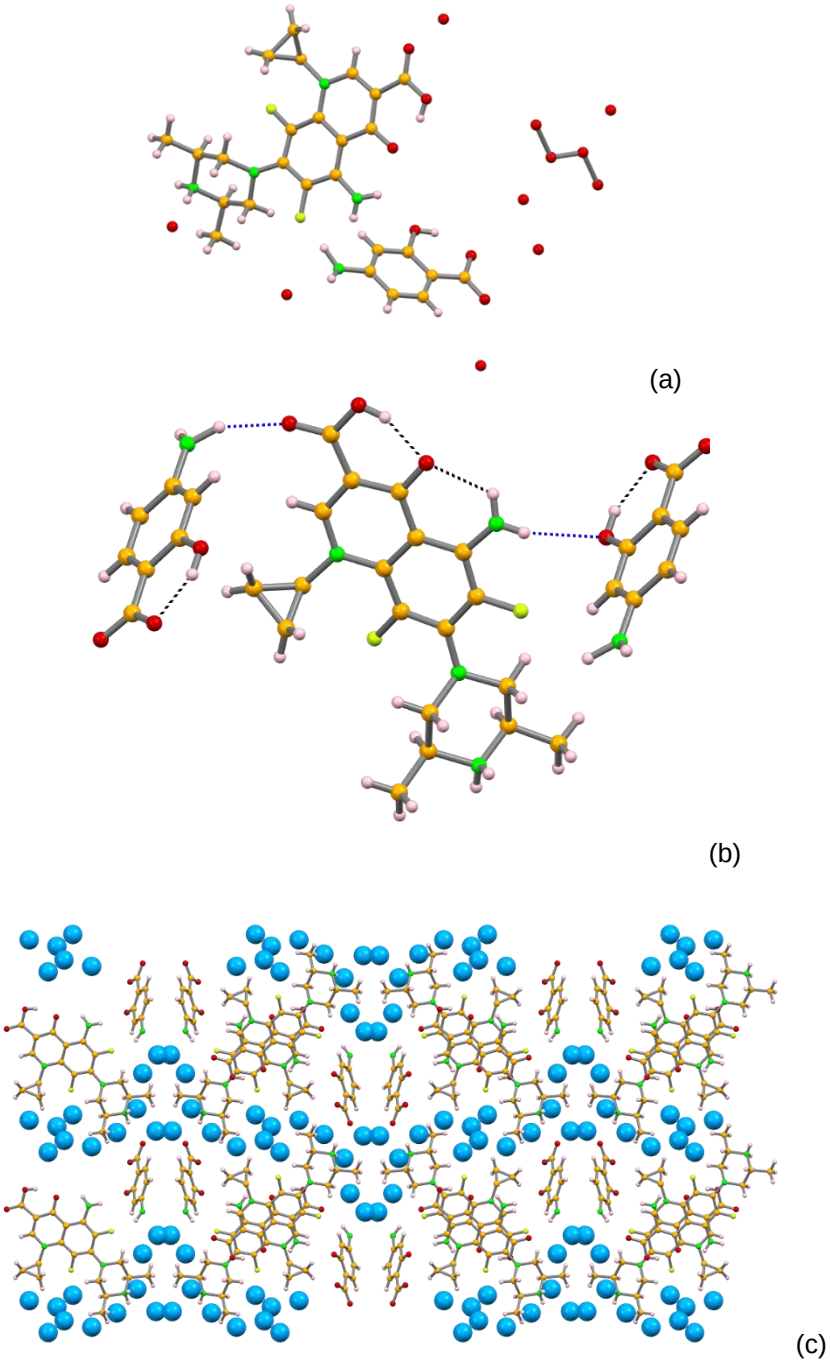

Figure 3-3 Illustration of **SPX:4ASA Form I** crystal structure depicting:: (a) the asymmetric unit with the disordered water cluster; (b) the intramolecular (black) and intermolecular (blue) hydrogen bonds established between SPX and 4ASA; and (c) the crystal packing of the Form I along the *a* axis Showing the water molecules in blue and using a spacefill representation

The asymmetric unit of **SPX:4ASA Form I** corresponds to one cationic SPX and one anionic 4ASA and a cluster with multiple disordered water molecules. The accurate number of water molecules was not possible to confirm by SCXRD. The typical intramolecular bonds in SPX established between the N-H_{NH2} and the carbonyl and the O-H_{COOH} and the carbonyl, as well as the intramolecular O-H_{COOH} ⋯ O_{OH} hydrogen bond of 4ASA are maintained. However, the N-H_{NH2} ⋯ O-H_{COOH} interactions between SPX is disrupted to give rise to interactions with 4ASA via N-$H_{NH2,SPX}$ ⋯ $O_{OH,4ASA}$ interactions (Figure 3-3).

Structural Characterization of SPX:4ASA Form II

Subsequent to the synthesis that led to the formation of **SPX:4ASA Form II** crystals, the PXRD measurement was performed. The comparison of the experimental PXRD pattern with the simulated pattern **SPX:4ASA Form II** obtained from the crystal structure data is represented in Figure 3-4.

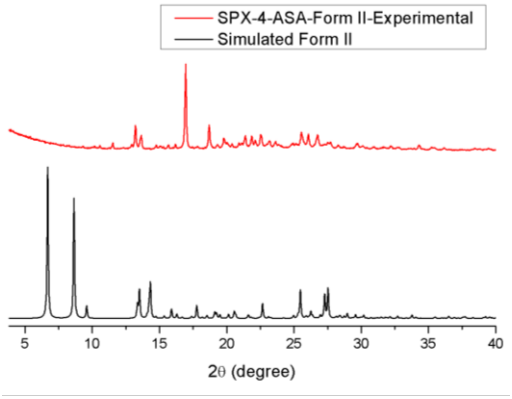

Figure 3-4 The comparison of the experimental PXRD patterns of the experimental bulk that yielded **SPX:4ASA Form II** with simulated **SPX:4ASA Form II** by SCXRD measurement

The PXRD result points out that **SPX:4ASA Form II** is not representative of the bulk of the initial experiment (Figure 3-4).

Bearing this unsuccessfull attemp in mind, the experimental conditions were changed. Subsequently, **SPX-4ASA-M-DMF** experimental procedure was performed. Later, PXRD measurement was performed for the experiment and the comparison of the PXRD pattern of the experimental procedure with the starting reagents as well as simulated **SPX:4ASA Form II** is shown in Figure 3-5.

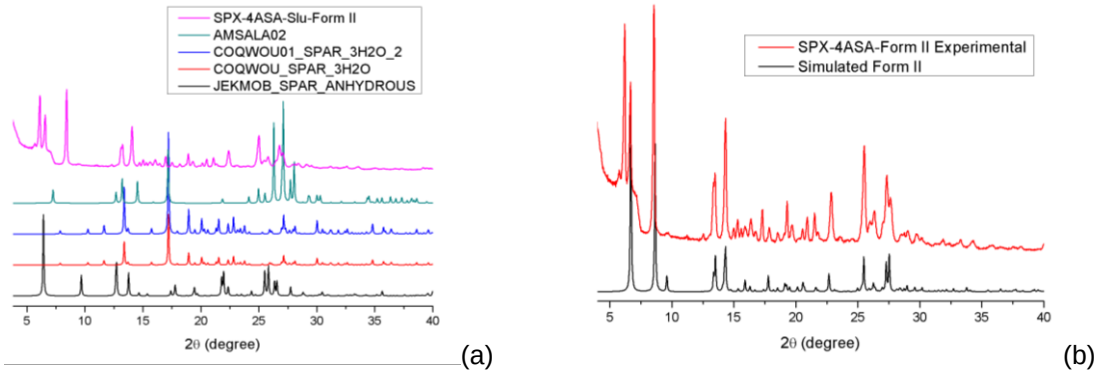

Figure 3-5 The comparison of the PXRD pattern of the experimental procedure of **SPX:4ASA Form II** with (a) starting reagents from CSD (b) **SPX:4ASA** Form II simulated from SCXRD data

According to the PXRD result, it can be mentioned that the PXRD patttern of experimental procedure is different from the starting reagents (Figure 3-5 (a)) whereas it is almost identical to the **SPX:4ASA Form II** (Figure 3-5 (b)) except the first peak appearing in the experimental PXRD pattern, and, therefore, further experiments must be done.

Additionally, TGA-DSC measurement was also porfermed. The result of TGA and DSC can be found in Figure 3-6.

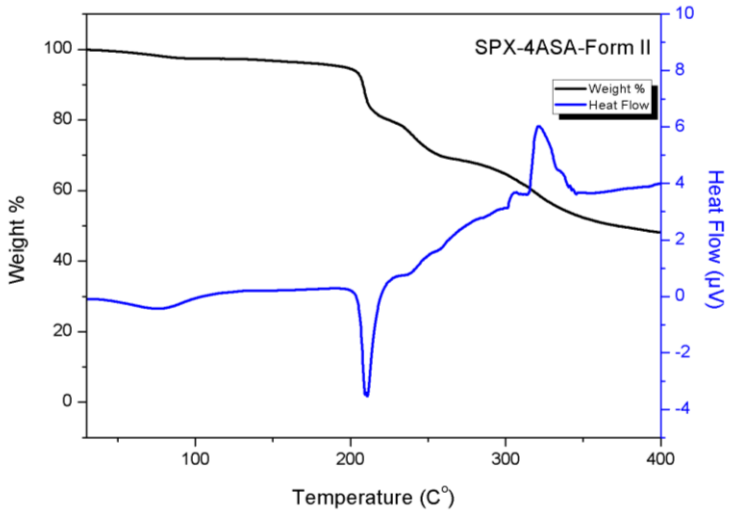

Figure 3-6 Thermogravimetric and DSC measurement result of **SPX:4ASA Form II**

According to the DSC and TGA results, it can be stated that melting and decomposition of **SPX:4ASA Form II** starts at 203°C. No mass loss is detected around 100°C, which confirms the anhydrous nature of this form.

Asides from the previous structural characterization methods, SCXRD measurement and crystal structure solution was also performed. The illustration of the asymmetric unit, intramolecular and intermolecular interactions as well as the crystal packing of **SPX:4ASA Form II** is shown in Figure 3-7.

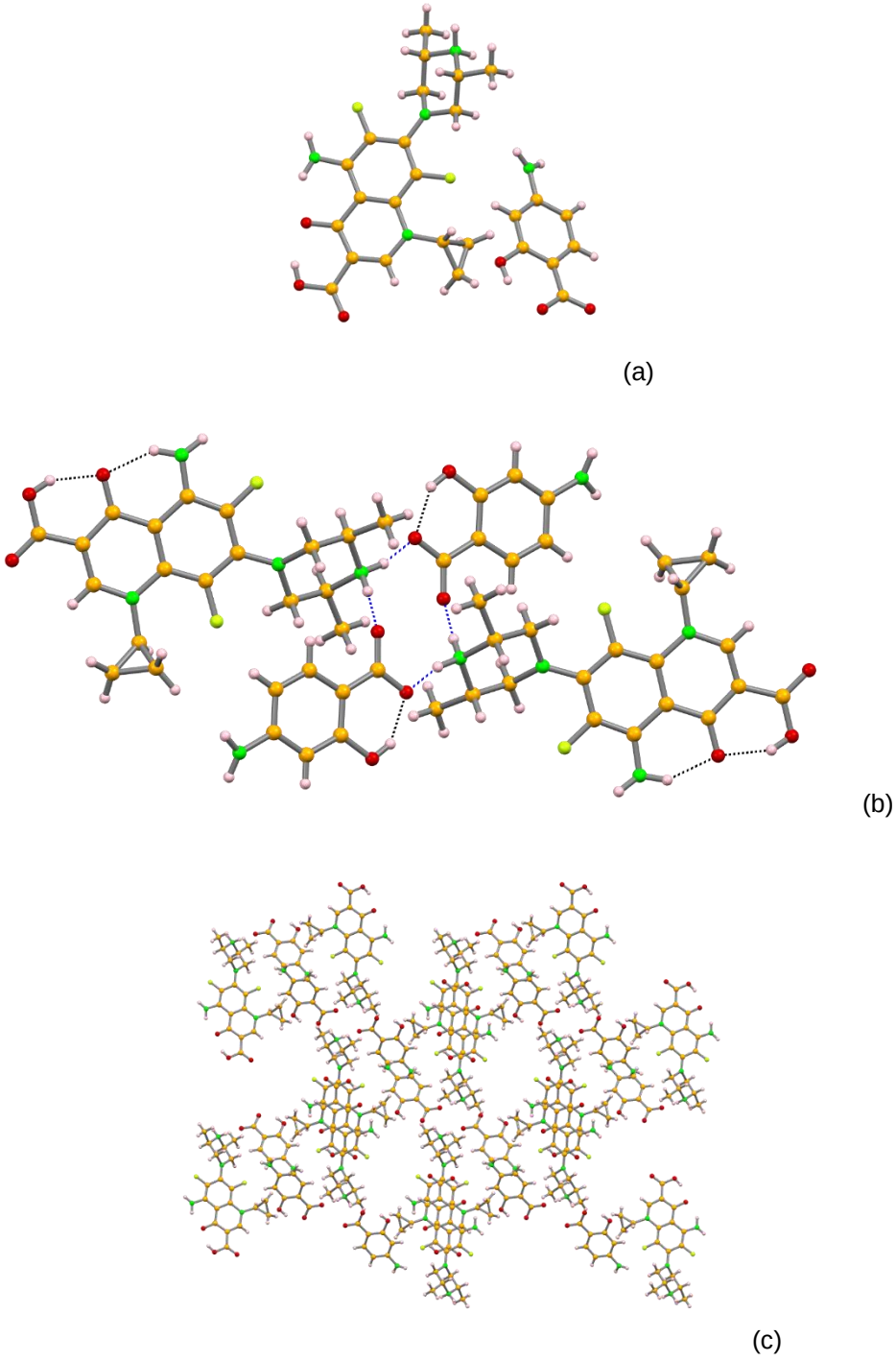

Figure 3-7 Illustration of Form II crystal structure depicting: (a) the asymmetric unit; (b) the intramolecular (black) and intermolecular (blue) interactions; and (c) the supramolecular arrangement in a view along the *b* axis

The asymmetric unit of **SPX:4ASA** Form II consists of one cationic SPX an one anionic 4ASA. The intramolecular interactions of both SPX and 4-ASA mentioned above are still maintained in the **SPX:4ASA Form II.** However, in this anhydrous form the interaction between 4ASA and SPX is established via the cationic NH_2^+ moiety of SPX. In a view along the *b* axis, the supramolecular arrangement shows a honey comb like packing (Figure 3-7 (c)). Further hydrogen bonding details of **SPX:4ASA Form II** are mentioned in Table 3-3.

Table 3-3 Hydrogen bonding details of **SPX:4ASA Form II**

Structure	(D)-H…A	Symmetry operator	D…A /Å	D…H /Å	H…A/ Å	D-H…A /º
SPX:4ASA Form II	N_2-H_1…O_3	x,y,z	2.639 (4)	0.90 (2)	1.87 (3)	143 (2)
	N_2-H_1…O_6	2-x, 1-y, 1-z	3.010 (4)	0.90 (2)	2.60 (4)	109 (3)
	O_2-H_{10}…O_3	x,y,z	2.506 (3)	0.82	1.75	152
	N_2-H_2…F_2	x,y,z	2.630 (4)	0.89 (3)	2.26 (4)	105 (3)
	O_6-H_6…0_5	x,y,z	2.523 (3)	0.82	1.79	147
	N_4-H_9…0_5	1/2+x, 1/2-y, -1/2+z	2.695 (4)	0.95 (3)	1.76 (3)	165 (3)
	N_4-H_{10}…0_4	3/2-x, 1/2+y, 3/2-z	2.744 (4)	0.86 (3)	1.89 (3)	175 (2)
SPX:4ASA Form II	C_{10}-H_{10}…0_1	x,y,z	2.787 (4)	0.93	2.45	101
	C_{14}-H_{14}…F_1	x,y,z	2.724 (4)	0.97	2.49	102
	C_{14}-H_{14}…O_2	2-x, 1-y, 1-z	3.340 (4)	0.97	2.33	147
	C_{17}-H_{17}…F_2	x,y,z	2.854 (3)	0.97	2.35	113

Apart from previous structural characterization methods, FTIR measurement was also made and the spectra of **SPX:4ASA Form II** is shown in Figure 3-8.

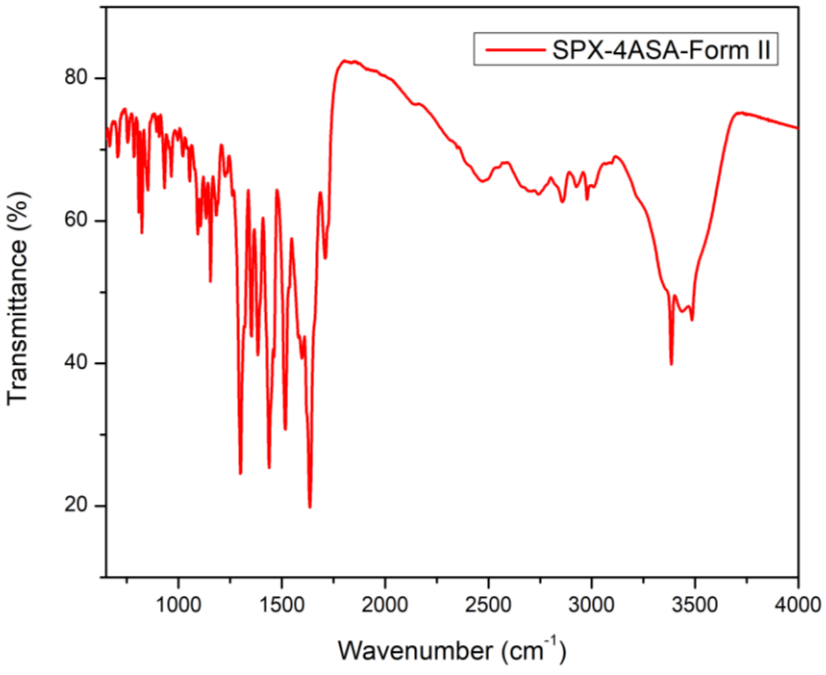

Figure 3-8 FTIR spectrum of **SPX:4ASA Form II**

The FTIR spectra of **SPX:4ASA Form II** shows the characteristic broadening around 3000 cm^{-1}, which might be attributed to the intramolecular and intermolecular hydrogen bonding of **SPX:4ASA Form II**. Additionally, the peak at 1517 cm^{-1} is related with the amine, as well as C=O asymmetric stretching at 1710 cm^{-1}, proving the salt formation. Apart from those peaks, monosubstituted C=C stretching peak at 1633 cm^{-1}, C-F stretching at 1300 cm^{-1} can also be found in the spectra. These peaks can be assigned to SPX whereas C-N stretching of amine at 1155 cm^{-1} can be assigned to both SPX and 4-ASA moities. Furthermore, OH bending of carboxylic acid can also be found at 1436 cm^{-1}.

Structural characterization SPX:4ASA Form III

Subsequent to the synthesis of **SPX:4ASA Form III**, the PXRD measurement was performed. The comparison of the experimental PXRD pattern with simulated **SPX:4ASA Form III** is represented in Figure 3-9.

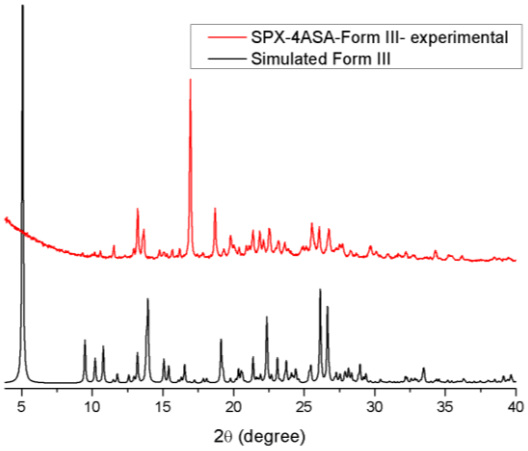

Figure 3-9 The comparison of experimental PXRD pattern with starting reagents and simulated **SPX:4ASA Form III**

The PXRD result points out that **SPX:4ASA Form III** is not representative of the experimental bulk (Figure 3-9). Bearing this unsuccessfull attemp in mind, the experimental conditions were changed. Subsequently, **SPX-4ASA(2:1)-M-ACN:EtOH** experimental procedure was perfomed. Afterwards, the PXRD measurement was performed. The comparison of the PXRD pattern of the experimental procedure with starting reagents as well as simulated **SPX:4ASA Form III** is shown in Figure 3-10.

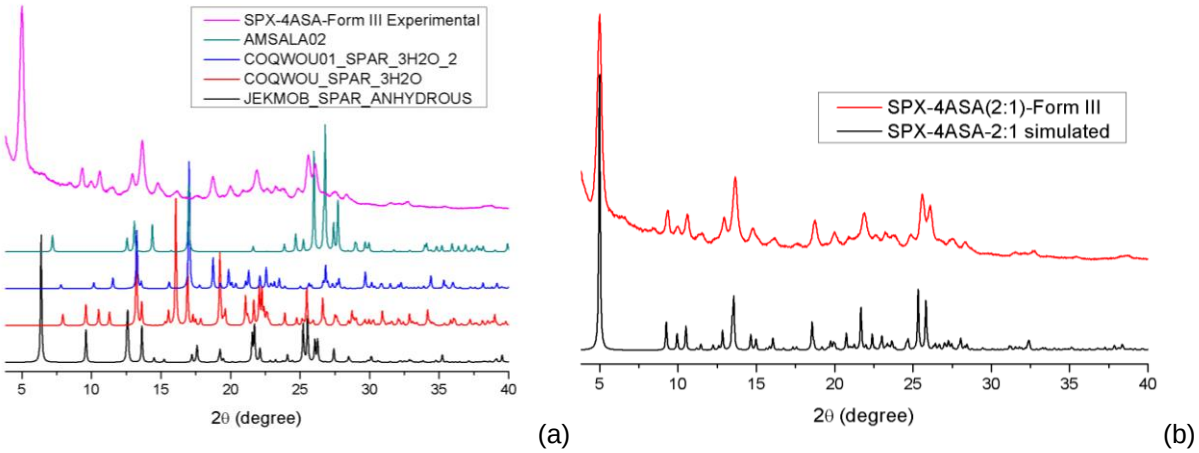

Figure 3-10 The comparison of experimental PXRD pattern of the experimental pattern with (a) starting reagents and (b) simulated **SPX:4ASA** Form III

According to the PXRD results, it can be stated that **SPX:4ASA Form III** is the representative of the experimental bulk, corresponding to a pure phase (Figure 3-10 (b)). The application of same solvent system but different synthesis method, manual grinding, resulted also in the pure phase formation of **SPX:4ASA Form III**. This result highlights the strength of mechanochemistry in the multicomponent screening of Sparfloxacin and 4-ASA.

Unfortunately, no single crystals with suitable quality for **SPX:4ASA Form III** were obtained, precluding a satisfactory refinement. However based in the bad quality SCXRD data acquired it is possible to say that this is a 2:1 (SPX:4ASA) hydrated form. For that reason, this study is an on-going process and hydrogen bonding details of this formare not mentioned within this study.

Physycochemical properties

Asides from the structural charactarization, it was aimed to further investigate the change in phsycochemical properties of the API such as stability and solubility. In this regard, the stability of **SPX:4ASA Forms II and III** were tested under 78% humidity atmosphere for 4 weeks by making the PXRD measurement each week. The stability test results of all forms are illustrated in Figure 3-11.

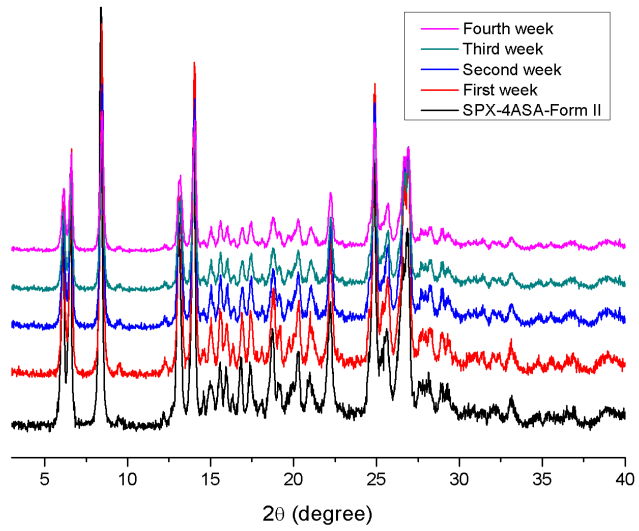

(a)

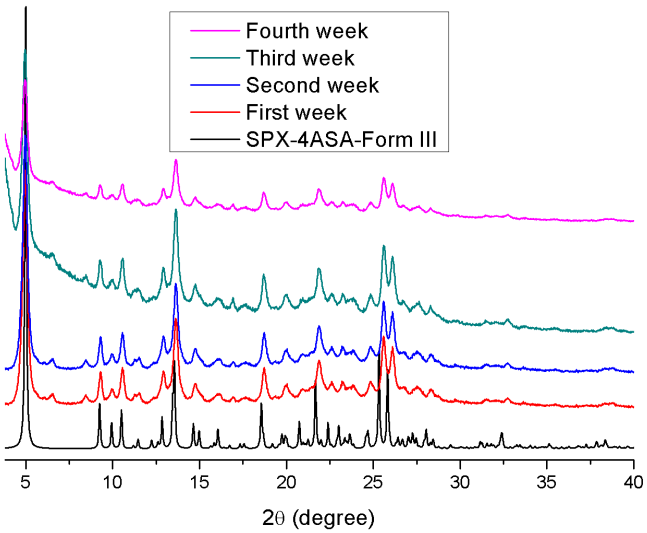

(b)

Figure 3-11 The comparison of PXRD diffractogram of (a) **SPX:4ASA Form II** and (b) **SPX:4ASA Form III** with the simulated multicomponent forms over four weeks

SPX:4ASA Forms II and III did not display change in PXRD diffractograms over 4 weeks, which points out the good stability behavior of the new forms. Therefore, it can be stated that the new multicomponent forms of SPX and 4-ASA are stale under 78% room humidity conditions for at least 4 weeks.

Lastly, the solubility tests of all multicomponent forms was made with an empirical bu result-oriented method. The change in the solubility is illustrated in Figure 3-12.

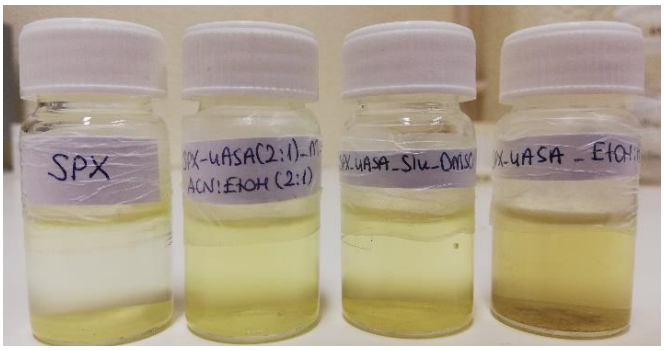

Figure 3-12 Solubility comparison of **SPX:4ASA Form I**, **I**I, **III**

On the basis of the solubility results shown in Figure 3.12, it can be mentioned that multicomponent screening of SPX with 4-ASA enhanced the solubility profile of the API. It is needed to note here that the nature of salt formation might be contributing to the solubility enhancement of the new forms. Asides from the comparison between SPX and new forms, a comparison between the multicomponent forms can also be done. As it can be seen from the figure, the most yellowish solution is **SPX:4ASA Form I**, which is the form with higher hydration level between the new forms obtained in this study. It is no surprise that this form reaches to the most soluble state. Hence, it is possible to conclude that the most soluble form is the **SPX:4ASA Form I** whereas the least soluble one looks like to be **SPX:4ASA Form III**. However, it is crucial to note that this method is empirical to make a reliable deduction. In order to fully investigate and ensure the solubility profile of the new the forms, HPLC studies are needed and these studies should be carried out not only in water but also in PBS, which mimicks the bloodstream more efficiently.

3.5.3 Multicomponent crystal forms screening with Sparfloxacin and 3-aminobenzoic acid

Throughout this study, 3-ABA was also used as co-former. The molecular structure of 3-ABA is shown in the Figure 3-13.

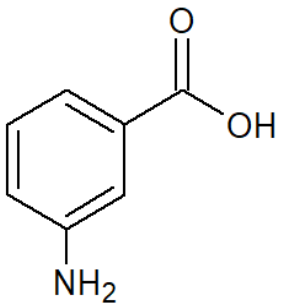

Figure 3-13 The molecular structure of 3-aminobenzoic acid (3-ABA)

As it can be seen, 3-ABA has two hydrogen bonding sites: aromatic carboxyl moiety, and aromatic amine (Figure 3-13) that are capable of contributing to the multicomponent formation. Considering the

active hydrogen bonding sites of SPX, it can be mentioned that there is high probabiliy of interactions with all substituents present in 3-ABA. In this study, the refcode of 3-ABA is used as AMBNZA03.

Herein, two different multicomponent form of SPX and 3-ABA were obtained. As provided by the theoretical expectations which indicates salt formation due to pKa difference between SPX[30] and 3-ABA[47] more than three units, salt formation was observed between the drug and the co-former in the newly obtained forms.

Structural Characterization

SPX:3ABA Form I

The **SPX:3ABA Form I** related PXRD patterns of experiment procedures compared with starting reagents as well as the simulated multicomponent form is shown in Figure 3-14.

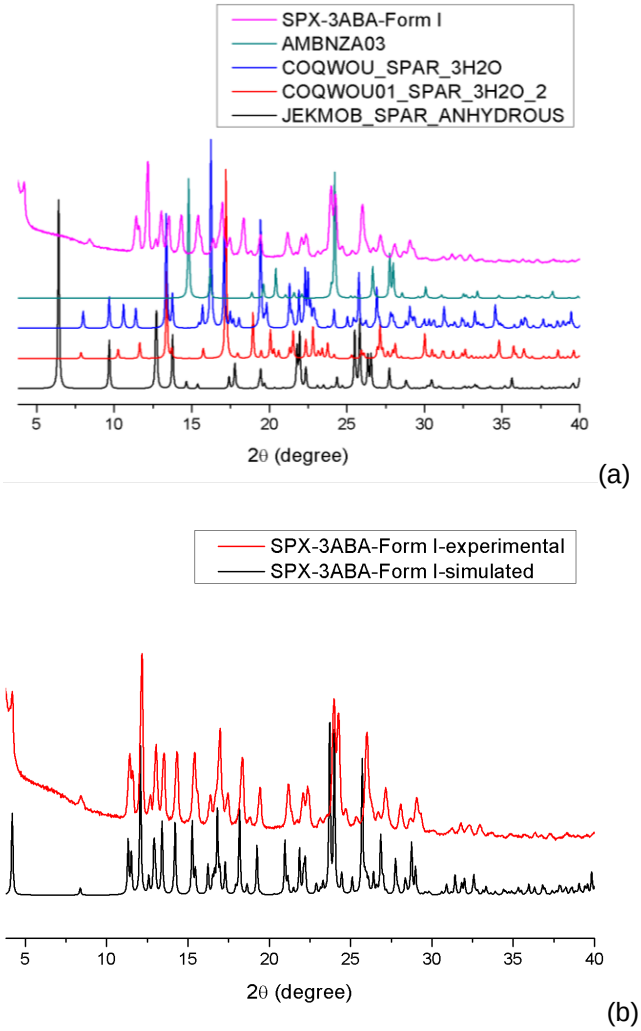

Figure 3-14 The comparison of PXRD patterns of experimental **3-ABA Form I** with (a) starting reagents (b) simulated **3-ABA Form I** by SCXRD

The PXRD shows that **SPX:3ABA Form I** as a pure phase.

To obtain further information about **SPX:3ABA Form I**, the crystal structure, which was previously determined,[51] is mentioned below. The asymmetric unit of the new form, intramolecular and intermolecular connection between SPX and 3-ABA, as well as crystal packing of **SPX:3ABA Form I**, is depicted in Figure 3-15.

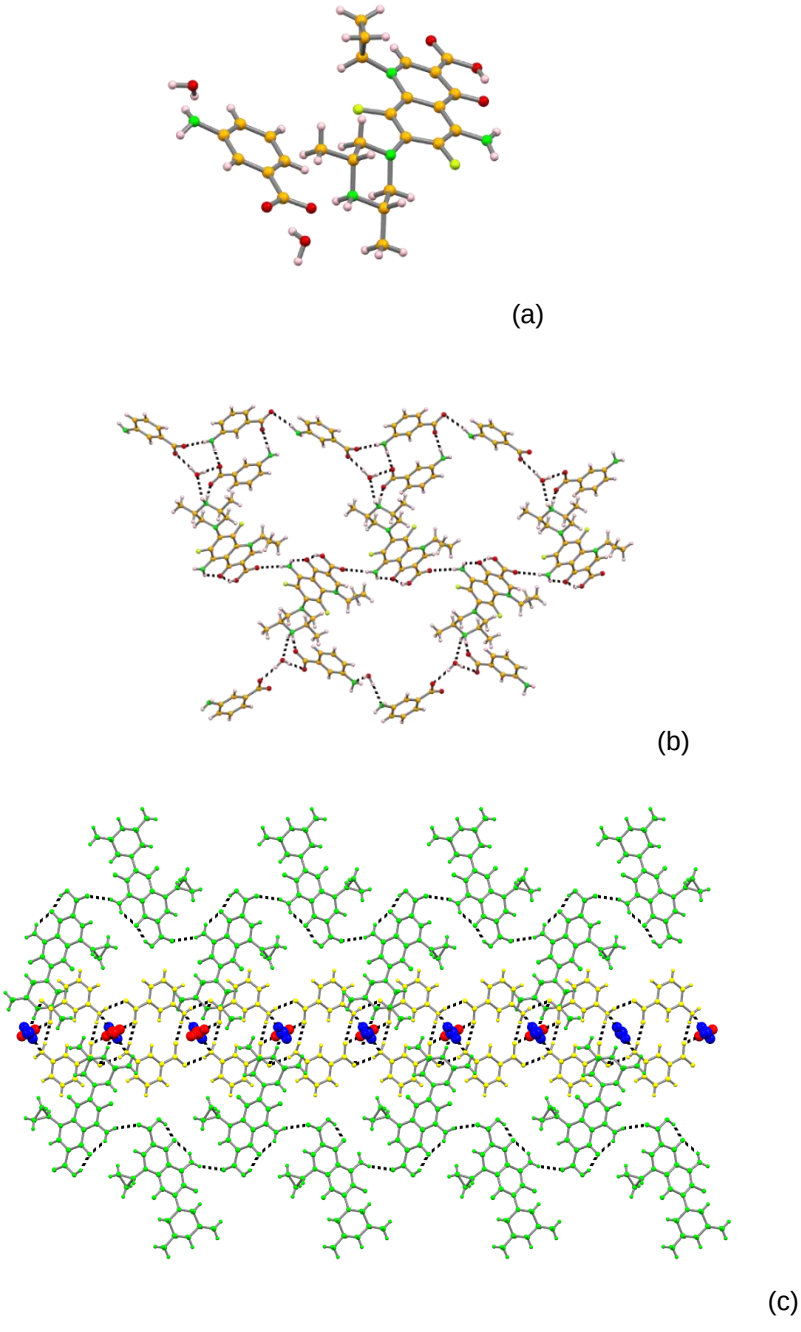

Figure 3-15 The illustration of SPX:3ABA Form I crystal structure depicting a) the asymmetric unit; b) the hydrogen bonding between SPX, 3ABA and water molecules; c) the crystal packing showing the zig-zag chains of SPX (green) intercalated with chains of 3ABA (yellow) and water molecules (red and blue, using spacefill representation)

The asymmetric unit of **SPX:3ABA Form I** involves one cationic SPX, one anionic 3-ABA and two water molecules. The typical intramolecular bonds in SPX are again maintained, as well as the N-H_{NH2} ⋯ O-

H_{COOH} interactions between SPX giving rise to zigzag chains. The interaction with 3ABA is established via the cationic NH_2^+ moiety (N-$H_{NH2+,SPX}$ ⋯ $O_{COO-,3ABA}$) and the water molecules (N-$H_{NH2+,SPX}$ ⋯ O-H_{H2O} ⋯ $O_{COO-,3ABA}$), giving rise to a supramolecular arrangement in wich zig-zag chains of SPX are alternated by a double layer of 3ABA and water molecules (Figure 3-15). Further hydrogen bonding details of **SPX:3ABA Form I** are stated below in Table 3-4.

Table 3-4 Hydrogen bonding details of **SPX:3ABA Form I**

Structure	**(D)-H…A**	**Symmetry operator**	**D…A /Å**	**D…H /Å**	**H…A/ Å**	**D-H…A /º**
Form I of 3-ABA co-former	O_1-H_1…0_3	x,y,z	2.534 (3)	0.892	1.77	153
	N_2-H_1…0_3	x,y,z	2.661 (3)	0.84 (3)	2.00 (3)	135 (3)
	O_1-H_1…N_5	x,y,z	2.942 (4)	0.90 (5)	2.10 (4)	174 (3)
	N_2-H_2…F_2	x,y,z	2.654 (3)	0.84 (3)	2.33 (3)	103 (2)
	N_2-H_2…0_2	1/2-x, 3/2-y, -1/2 z	3.052 (4)	0.86 (3)	2.24 (3)	159 (3)
	O_2-H_2…0_4	1-x, y, 1/2-z	2.777 (3)	0.86 (3)	1.90 (3)	175 (4)
	N_4-H_3…0_2	x,y,z	2.857 (3)	0.88 (4)	2.24 (3)	121 (2)
	N_4-H_3…0_1	1-x, 1-y, 1-z	2.917 (3)	0.96 (3)	2.10 (3)	142 (3)
	N_4-H_4…0_5	x,y,z	2.747 (4)	0.92 (3)	1.84 (3)	166 (2)
	N_5-H_5…0_4	1-x, -y, 1-z	3.010 (4)	0.93 (3)	2.09 (3)	172 (3)
	N_5-H_6…O_5	x, -y, 1/2+z	3.104 (3)	0.88 (3)	2.24 (3)	166 (3)
	C_{10}-H_{10}…0_2	x,y,z	2.787 (3)	0.93	2.45	102
	C_{12}-H_{12}…0_2	1/2-x, 1/2+y,z	3.412 (5)	0.97	2.54	150
	C_{14}-H_{14}…F_2	x,y,z	2.896 (4)	0.97	2.28	121
	C_{14}-H_{14}…0_5	x,y,z	3.312 (4)	0.97	2.60	131
	C_{22}-H_{22}…0_4	x,y,z	2.770 (3)	0.93	2.45	100

For further structure characterization, FTIR measurement was also performed. The experimental spectrum of the **SPX:3ABA Form I** is shown in Figure 3-16.

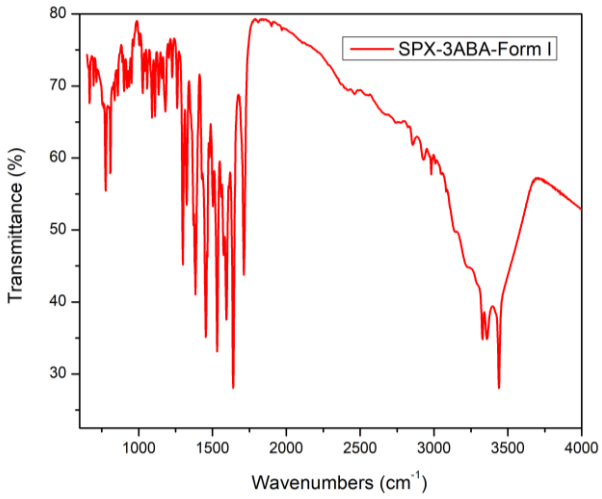

Figure 3-16 FTIR spectrum of **SPX:3ABA Form I**

The FTIR spectra of experimental **SPX:3ABA Form I** shows the characteristic broadening around 3000 cm^{-1}, which might be attributed to the intramolecular and intermolecular hydrogen bonding of **Form I**. Additionally, the peak at 1531 cm^{1} is related with the amine and the C=O asymmetric stretching at 1710 cm^{-1} indicates salt formation. Apart from those peaks, monosubstituted C=C stretching peak at 1633 cm^{-1}, C-F stretching at 1384 cm^{1} can also be found in the spectra. These peaks can be assigned to SPX whereas C-N stretching of amine at 1089 cm^{-1} can be assigned to both SPX and 3-ABA molecules.

Moreover, TGA-DSC measurement was also performed and the result is illustrated below.

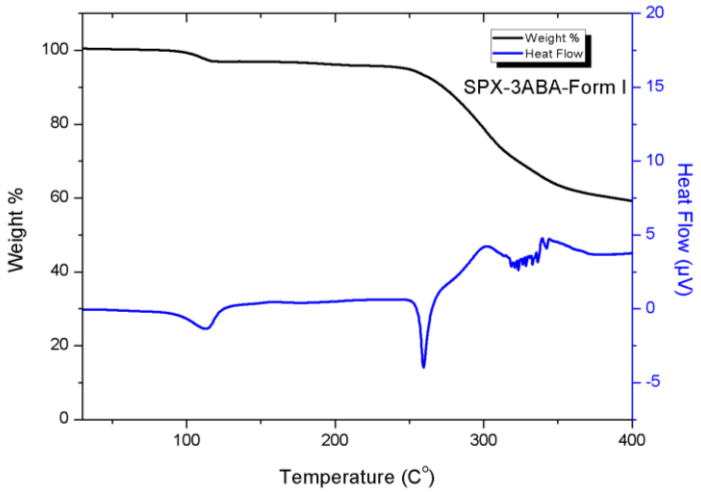

Figure 3-17 TGA-DSC spectrum of **SPX:3ABA Form I**

The DSC and TGA data for a pure sample of SPX:3ABA Form I shows an endothermic event associated

with approximately 3% of mass loss at 114 °C. This value of mass loss is in good agreement with the expected water loss, according to its crystal structure. Furthermore, melting and decomposition of the **SPX:3ABA Form I** starts at around 252 °C.

SPX:3ABA Form II

The comparison of PXRD patterns of experimental procedure of **SPX:3ABA Form II** with starting reagents and the simulated multicomponent form is shown in Figure 3-18.

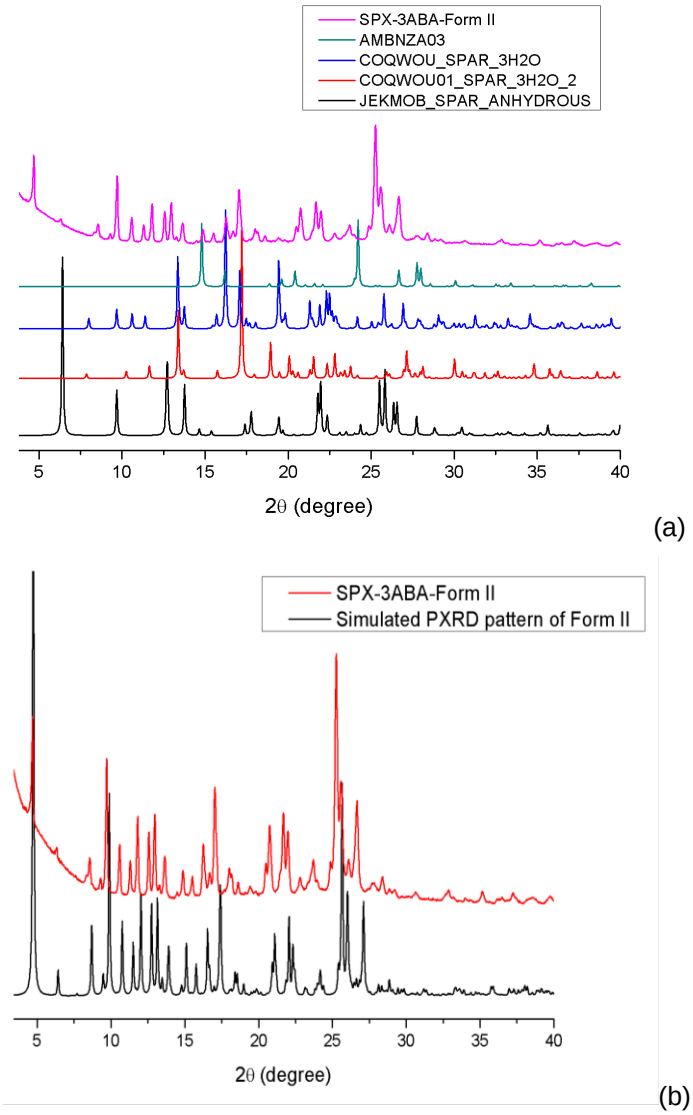

Figure 3-18 The comparison of PXRD patterns of experimental **SPX:3ABA** Form II with (a) starting reagent (b) the simulated multicomponent form

PXRD data proves the formation of **SPX:3ABA Form II** as a pure phase.

To obtain further information about **SPX-3ABA Form II**, its crystal structure, which was previously determined within the group,[51] is mentioned below. The asymmetric unit, intramolecular and

intermolecular hydrogen bonding, as well as crystal packing of **SPX:3ABA Form II**, can be found in Figure 3-19.

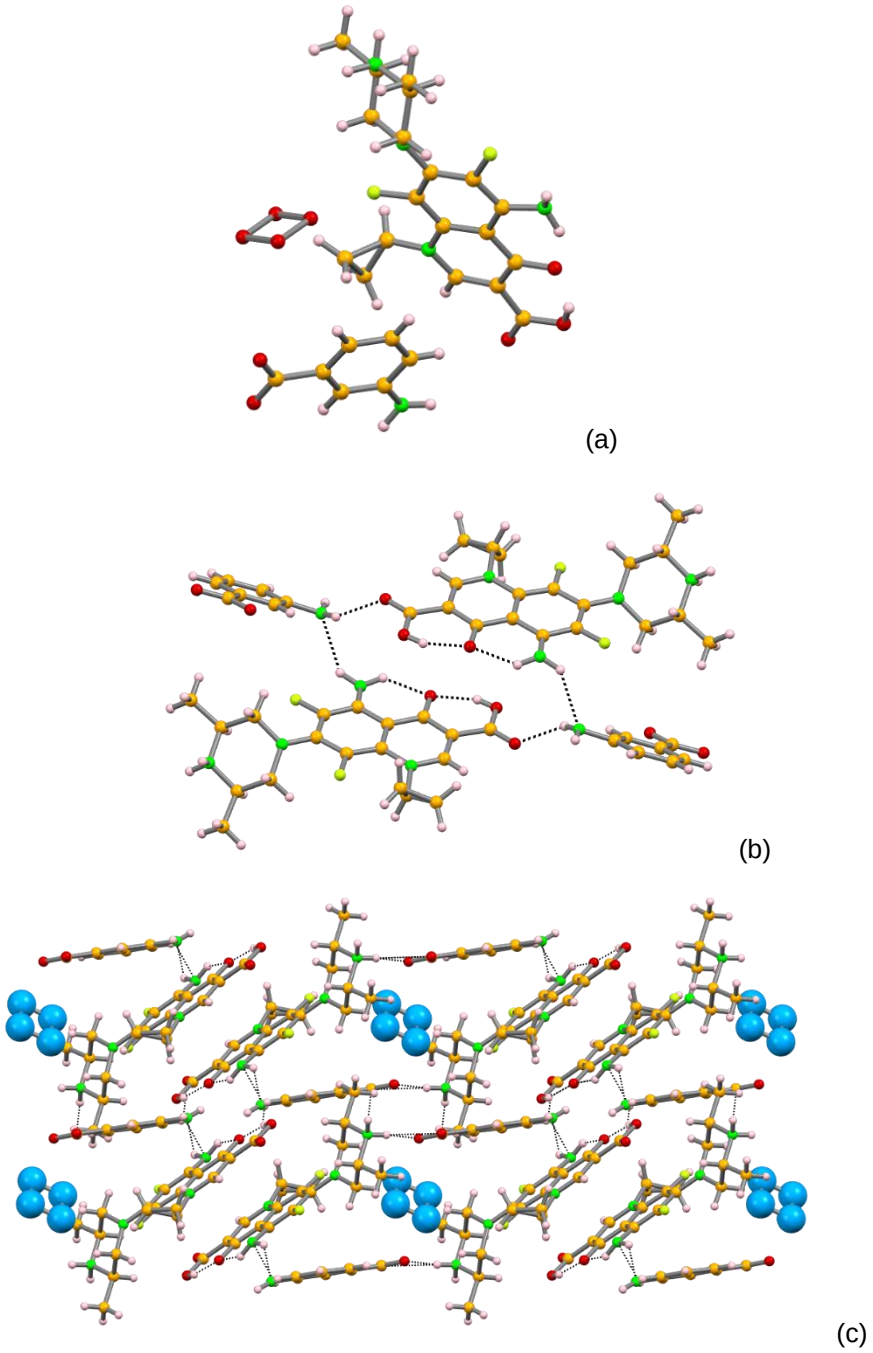

Figure 3-19 The illustration of **SPX:3ABA** Form II crystal structure depicting (a) the asymmetric unit; (b) the hydrogen bonding between SPX and 3ABA; (c) the crystal packing showing the ladder-like chains of 3ABA separate rows of SPX and water clusters (blue)

The asymmetric unit of Form II involves one cationic SPX, one anionic 3-ABA and a disordered water cluster residing over a special position. The typical intramolecular bonds in SPX are again maintained, but the N-H_{NH2} ⋯ O-H_{COOH} interactions is disrupted to give rise to the interaction with 3-ABA(N-$H_{NH2,SPX}$⋯$N_{NH2,3\text{-}ABA}$ and N-$H_{NH2,3ABA}$ ⋯$O_{COOH,SPX}$). In the overall supramolecular packing, it is possible to see ladder-like chains of 3-ABA, separate rows of SPX, and water clusters (Figure 3-19). Further

hydrogen bonding details of **SPX:3ABA Form II** is stated in Table 3-5.

Table 3-5 Hydrogen bonding details of **SPX:3ABA Form II**

Structure	(D)-H…A	Symmetry operatör	D…A /Å	D…H / Å	H…A/ Å	D-H…A / º
Form II of 3-ABA co-former	N_2-H_1…F_2	x,y,z	2.628 (4)	0.91 (2)	2.19 (3)	109 (2)
	N_2-H_1…N_5	x, 1+y, z	3.206 (5)	0.91 (2)	2.45 (4)	140 (3)
	O_1-H_1…O_3	x,y,z	2.505 (3)	0.82	1.75	153
	N_2-H_2…0_3	x,y,z	2.642 (4)	0.89 (3)	1.95 (4)	134 (3)
	N_4-H_3…0_4	1+x, 1+y, z	2.678 (5)	0.91 (4)	1.77 (4)	172 (4)
	N_4-H_4…0_4	1-x, 1-y, -z	3.297 (4)	0.93 (3)	2.57 (3)	136 (3)
	N_4-H_4…0_5	1-x, 1-y, -z	2.742 (4)	0.93 (3)	1.83 (3)	168 (3)
	N_4-H_4…0_5	x,-y, 1-z	3.027 (5)	0.91 (5)	2.30 (3)	137 (7)
	N_5-H_5…0_2	x,y,z	2.790 (4)	0.89 (4)	2.46	101
	C_{10}-H_{10}…0_2	x,y,z	2.797 (4)	0.97	2.24	115
	C_{14}-H_{14}…F_2	x,y,z	2.704 (4)	0.97	2.24	108
	C_{22}-H_{22}…O_4	x,y,z	2.774 (4)	0.93	2.46	100
	C_{24}-H_{24}…O_3	x, 1-y, 1-z	3.362 (4)	0.93	2.60	140

For further structural characterization, FTIR measurement was also performed. The experimental spectrum of **SPX:3ABA Form II** is shown in Figure 3-20.

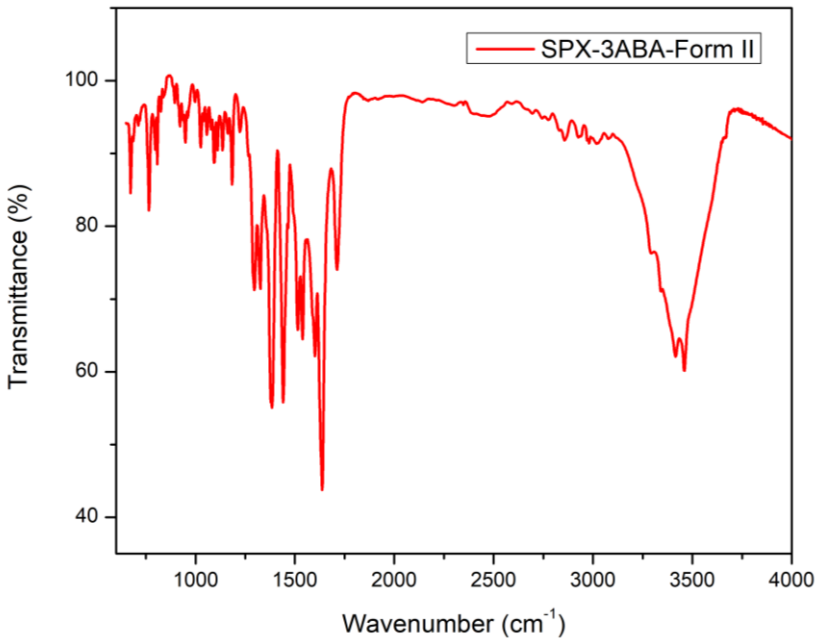

Figure 3-20 FTIR spectrum of **SPX:3ABA Form II**

The FTIR spectra of experimental **SPX:3ABA Form II** shows the characteristic broadening around 3000 cm^{-1}, which might be attributed to the intramolecular and intermolecular hydrogen bonding of **SPX:3ABA Form II**. Additionally, the peak at 1537 cm^{1} is related with the amine and the C=O asymmetric stretching at 1710 cm^{-1} confirm the salt formation.Apart from those peaks, monosubstituted C=C stretching peak at 1633 cm^{-1}, C-F stretching at 1384 cm^{1} can also be found in the spectra. These peaks can be assigned to SPX whereas C-N stretching of amine at 1184 cm^{-1} can be assigned to both SPX and 3-ABA molecules.

Moreover, TGA-DSC measurement was also perfomed for **SPX:3ABA Form II**. The result of the measurement is shown in Figure 3-21.

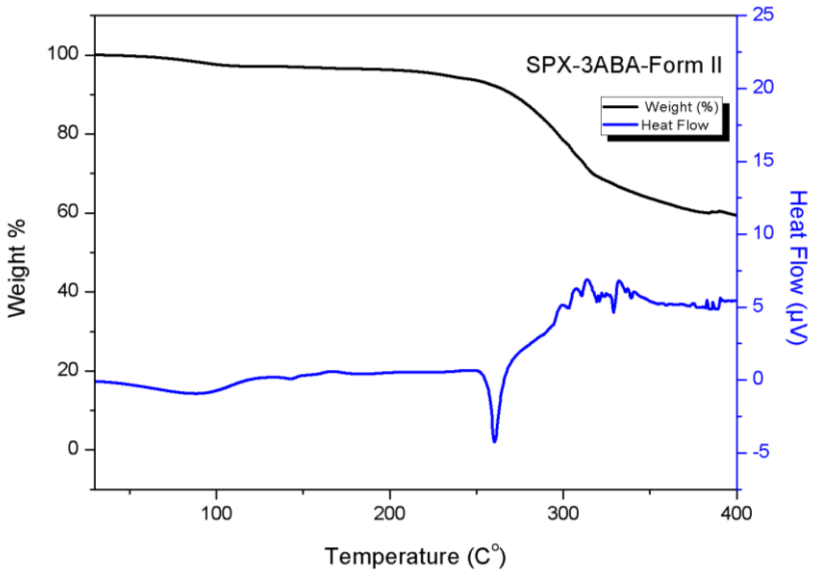

Figure 3-21 The result of TGA-DSC measurement of **SPX:3ABA Form II**

The DSC and TGA data for a pure sample of **SPX:3ABA Form II** shows an endothermic event associated with approximately 3% of mass loss at 103 °C. The approximately 3% of mass loss indicates that the disordered water cluster corresponds to a total of two water molecules. Furthermore, melting and decomposition of **SPX:3ABA Form II** starts at around 250 °C.

Physicochemical Properties

In addition to the structural characterization of **SPX:3ABA Form II Form I** and **Form II**, physicochemical properties such as stability and solubility was also studied.

To start with stability, the newly obtained two forms were exposed to 78% humidity atmosphere for 4 weeks and each week the change in the structure was investigated by PXRD. The results of the stability study are demonstrated in Figure 3-22.

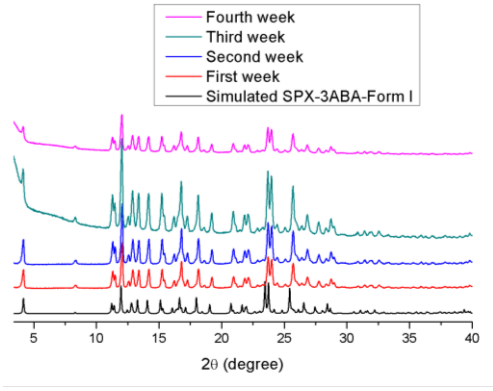

(a)

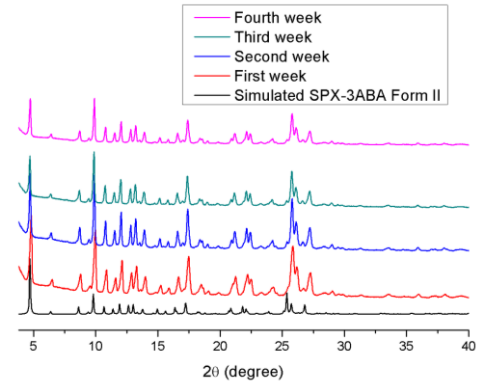

(b)

Figure 3-22 The comparison of PXRD diffractograms of a) **SPX:3ABA Form I** and b) **SPX:3ABA Form II** under 78% of humidity for 4 weeks with simulated multicomponent form

The PXRD diffractograms illustrate no changes in both **SPX:3ABA Forms I and II,** which is a proof of its stability under these circumstances. In this sense, it can be stated that both **SPX:3ABA Forms I** and **II** are stable under 78% humidity atmosphere for at least 4 weeks.

Besides the stability studies, also the solubility profile with an empirical method was estimated. The

comparison of solubility difference between **SPX:3ABA Forms I** and **II** with SPX is illustrated in Figure 3-23.

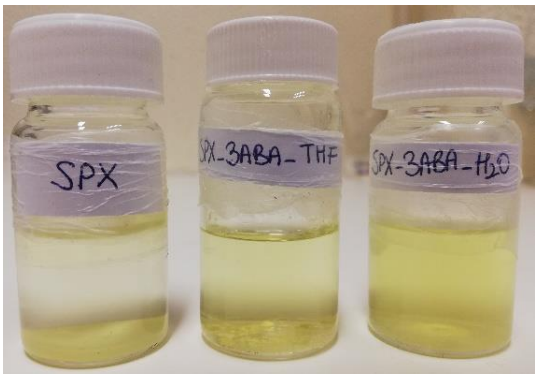

Figure 3-23 The solubility behavior of **SPX:3ABA** Form I and **SPX:3ABA** Form II compared with Sparfloxacin

As it can be seen from the figure, the solubility of SPX in water is highly limited. Both **SPX:3ABA** forms are more soluble than SPX. When it comes to compare the solubility behaviour of both forms with 3-ABA, it can be stated that **SPX:3ABA Form II** has higher solubility. Here it is need to note that **Form II** has a higher hydration level than **SPX:3ABA Form I**. This fact might be contributing to the solubility behaviour of the **SPX:3ABA Form II**. However, similarly to what was previously said for the systems with 4ASA, this method is empirical. In order to fully investigate and ensure the solubility profile of the new forms, a HPLC study is needed to test solutions not only in water but also in PBS, which mimics the bloodstream more efficiently.

3.5.4 Multicomponent crystal forms screening with Sparfloxacin and Anthranilic acid

Another applied co-former was the Anthranilic acid (AA). The molecular structure of AA is shown in Figure 3-24.

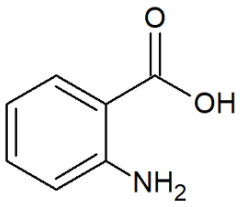

Figure 3-24 Molecular structure of Anthranilic acid

Anthranilic acid has two hydrogen bonding sites: an aromatic carboxylate and an aromatic NH_2 (Figure 3-24). Both these functional groups are capable of providing hydrogen bonding with SPX.

The use of AA as a co-former resulted in the formation of one multicomponent form (**SPX:AA**). Based on previous attempts of the research group, the experimental conditions were repeated to enhance the quality of the multicomponent form. Yet, there was no improvement in the quality of crystals obtained with SPX and AA.

Like other multicomponent forms of SPX, this multicomponent form is also a salt. This fact might be attributed to more than three unit difference in pKa difference between SPX[30] and AA[46] but also it should be noted that AA has two hydrogen bonding groups on ortho position, which may lower the acidity and basicity behaviour of the active sites.

Structural characterization of SPX:AA

The comparison of the PXRD pattern of the experimental procedure with starting reagents and simulated multicomponent form is demonstrated in Figure 3-25.

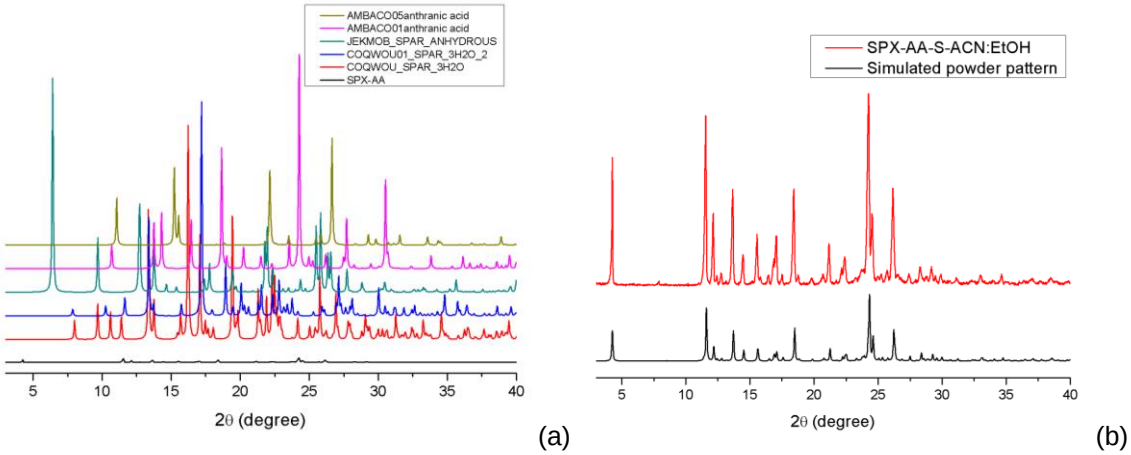

Figure 3-25 Comparison of the experimental diffractogram of **SPX-AA** multicomponent form with (a) starting reagents (b) simulated multicomponent form

PXRD data shows that pure **SPX:AA** was obtained as a pure phase. Yet no better quality single crystals were grown.

For further structural information, the crystal structure of **SPX:AA** previously determined within the group is mentioned below.The illustration of the asymmetric unit, intramolecular and intermolecular hydrogen bonding as well as crystal packing of the new multicomponent form is shown in Figure 3-26.

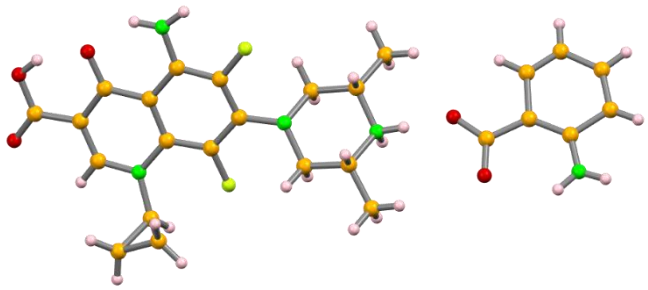

(a)

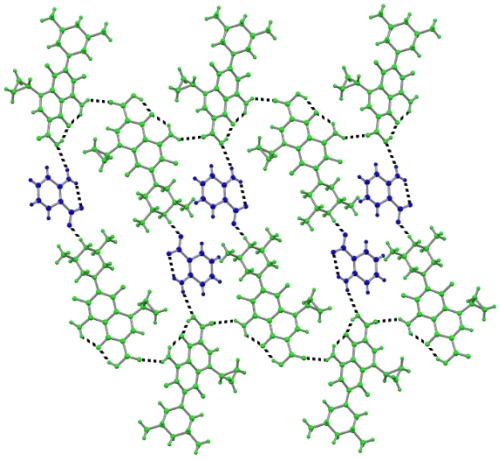

(b)

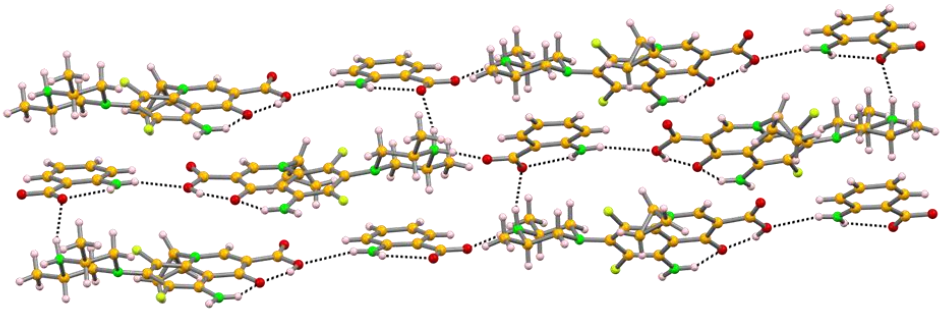

(c)

Figure 3-26 The illustration of **SPX:AA** crystal structure depicting a) the asymmetric unit; b) the hydrogen bonding between SPX and AA (blue); c) the crystal packing showing the alternance between SPX and AA

The asymmetric unit of SPX and AA salt contains one cationic SPX and one anionic AA. The typical intramolecular bonds in SPX are maintained, as well as the zigzag chains formed by the N-H_{NH2} ⋯ O-H_{COOH} interactions between SPX. The interaction with AA is established via the cationic moiety of SPX (N-$H_{NH2+,SPX}$ ⋯ $O_{COO-,AA}$) and also by the NH_2 moiety of AA and the carboxylic group of SPX (N-$H_{NH2,AA}$ ⋯ O-$H_{COOH,SPX}$). In the overall packing, the zig-zag chains of SPX alternate with AA, without any hydrogen bond being established between AAs (Figure 3-26). The hydrogen bonding details are stated in Table 3-6.

Table 3-6 Hydrogen bonding details of **SPX:AA**

Structure	(D)-H…A	Symmetry operator	D…A /Å	D…H /Å	H…A/ Å	D-H…A /º
SPX-AA	N_2-H_1…0_3	x,y,z	2.627 (8)	0.89 (3)	1.90 (5)	137 (5)
	O_2-H_2…0_3	x,y,z	2.510 (7)	0.82	1.75	154
	N_2-H_2…F_2	x,y,z	2.658 (8)	0.90 (5)	2.19 (5)	112 (4)
	N_2-H_2…0_1	1-x, 1/2+y, 1/2-z	2.976 (9)	0.90 (5)	2.25 (5)	137 (4)
	N_4-H_3…0_4	x,,y,z	2.643 (9)	0.90 (5)	1.75 (5)	176 (8)
	N_4-H_4…0_5	x,y,z	2.785 (10)	0.89 (3)	1.93 (3)	161 (6)
	N_5-H_5…0_5	x,y,z	2.895 (13)	0.86	2.30	126
	N_5-H_5…0_5	x, 3/2-y, ½+z	3.424 (11)	0.86	2.59	164
	C_{10}-H_{10}…0_1	x,y,z	2.792 (8)	0.93	2.46	101
	C_{12}-H_{14}…0_1	-1/2+x, y, 1/2-z	3.376 (10)	0.97	2.54	145
	C_{14}-H_{14}…F_2	x,y,z	2.88 (9)	0.97	2.27	120
	C_{26}-H_{26}…0_4	x,y,z	2.666 (13)	0.93	2.34	101

Apart from this structural characterizations, FTIR measurement was also performed. The related spectrum of FTIR is shown in Figure 3-27.

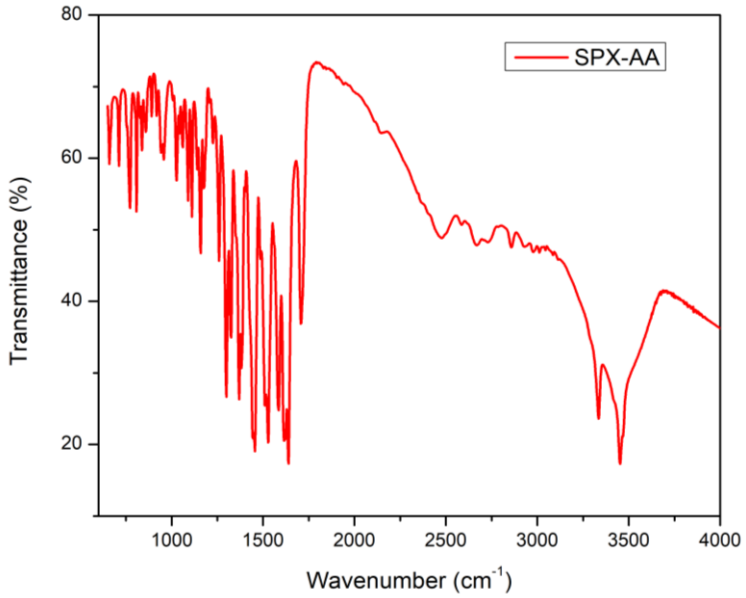

Figure 3-27 The FTIR spectrum of **SPX:AA**

The FTIR spectra of SPX and AA multicomponent form shows the characteristic broadening around 3000 cm^{-1}, which might be attributed to the intramolecular and intermolecular hydrogen bonding of multicomponent form. Additionally, the peak at 1529 cm^{-1} related with the amine and the C=O asymmetric stretching at 1706 cm^{-1} prove the salt formation.

Apart from those peaks, monosubstituted C=C stretching peak at 1641 cm^{-1}, C-F stretching at 1369 cm^{1} can also be found in the spectra. These peaks can be assigned to SPX whereas C-N stretching of amine at 1157 cm^{-1} can be assigned to both SPX and AA molecules (Figure 3-27).

Furthermore, TGA-DSC measurement was also performed for the multicomponent form of Sparfloxacin and Anthranilic acid. The result is demonstrated in Figure 3-28.

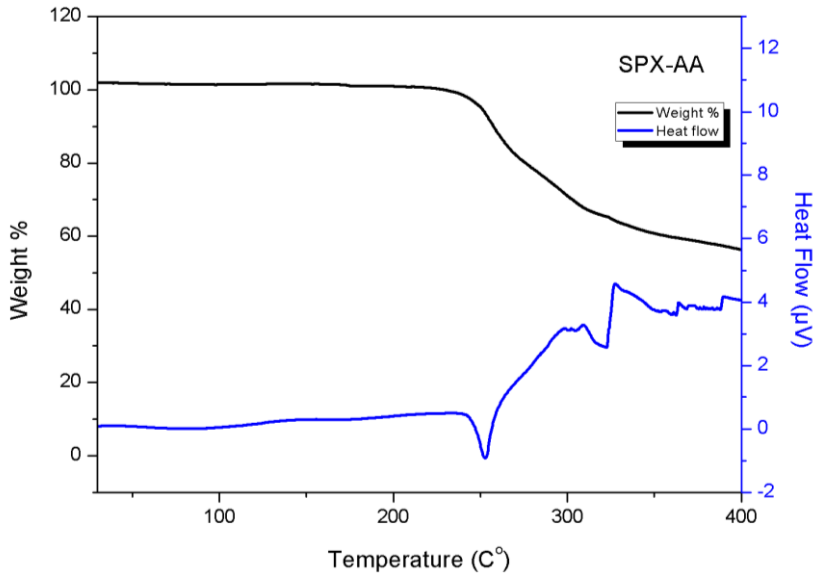

Figure 3-28 The TGA-DSC graph of **SPX:AA**

DSC and TGA data of **SPX:AA** show that this salt melts and decomposes at 240 °C. Furthermore, no mass loss is detected around 100°C, confirming the absence of water in the crystal structure determined from SCXRD data.

Physicochemical properties

In order to observe the changes in the physicochemical properties of the API, stability and solubility behaviour were tested for **SPX:AA**.

To start with, the stability behaviour of this form was tested by exposing the new form to 78% humidity atmosphere for 4 week. The PXRD measurement was performed each week and the related PXRD diffractograms compared with its simulated data are shown in Figure 3-29.

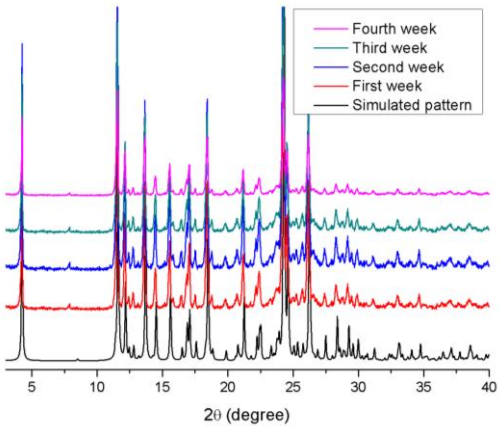

Figure 3-29 The stability comparison of Sparfloxacin and Anthranilic acid multicomponent form under 78% humidity atmosphere for 4 weeks

The PXRD diffractograms of **SPX:AA** allow to conclude that the new multicomponent form has stability at least for 4 weeks under 78% humidity room temperature (Figure 3-29).

Apart from the stability, solubility behaviour of the multicomponent form was also analysed with an empirical method. The solubility difference between SPX and **SPX:AA** is illustrated in Figure 3-30.

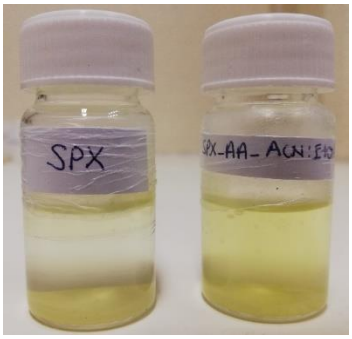

Figure 3-30 The comparison of solubility behaviour of Sparfloxacin (left) and **SPX:AA** (right)

According to the solubility profile shown in Figure 3-30, it can be stated that **SPX:AA** boosted the

solubility of SPX.The reason for the enhancement in the solubility might be attributed to the extra hydrogen bonding sites, which ultimately improves the solubility behaviour in water. Further solubility tests in water and PBS, using HPLC data are needed to complement this study.

3.5.5 Multicomponent crystal forms screening with Sparfloxacin, Nalidixic acid and 4-aminosalicylic acid multicomponent form

Over the successful attempts of combination of SPX and 4-ASA, our research interest has been shifted to formation of a three antibiotic multicomponent form. For that reason, nalidixic acid and 4ASA were chosen as co-formers in addition to SPX.

Inspired by the successful results of mechanochemistry for the formation of SPX-4ASA forms, the priority was given to this technique. The PXRD diffractogram of **SPX-NA-4-ASA-M-ACN:EtOH** experimental procedure led to the formation of a new multicomponent form. The comparison of PXRD pattern of experimental procedure with starting reagents are shown in Figure 3-31.

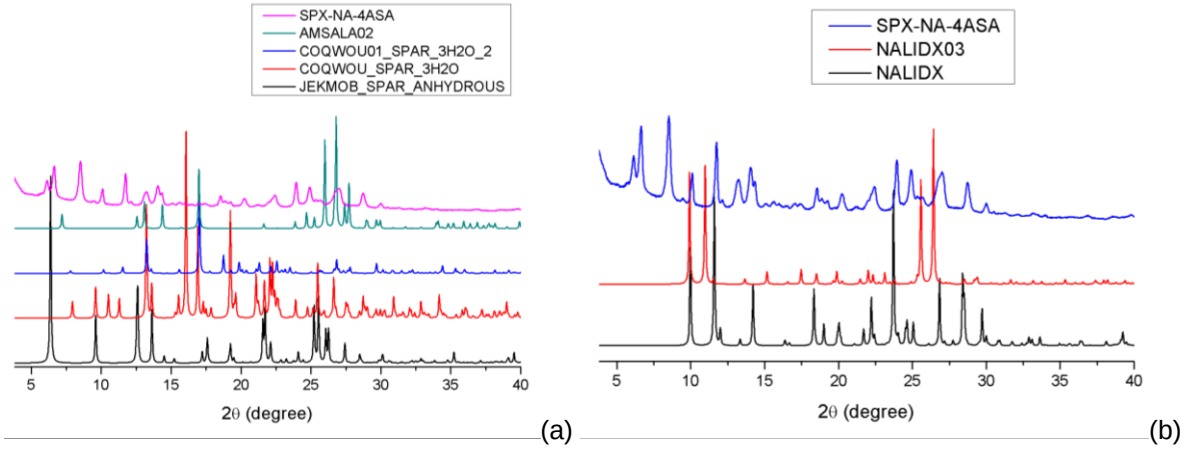

Figure 3-31 The comparison of PXRD pattern of experimental procedure with starting reagents from CSD database; (a) Sparfloxacin and 4-aminosalycylic (b) Nalidixic acid

According to the PXRD results, the formation of a new form with SPX, NA and 4-ASA can be concluded since the PXRD pattern of the experimental procedure is different from starting reagents (Figure 3-31 (a) and (b)). However, due to unsuccessful attempts of recrystallization of this form, the crystal structure is still unknown and remains as an on-going research. Yet, it can still be mentioned that we were most likely successful in the formation of a new form enclosing simultaneously SPX, NA and 4-ASA by the use of manual grinding.

Due to the lack of structural data, no further structural characterization was applied for this form.

3.6 Conclusion

To sum up, six different salts of SPX were synthesized by slow evaporation, manual grinding and slurry reactions. The use of a variety of experimental techniques was essentially important throughout the investigation of multicomponent forms of SPX in order to obtain pure-phase production of the salts.

Throughout this study, it is shown that the salt formation over co-crystal is favored between SPX and the explored co-formers studied herein, namely 4-ASA, 3-ABA, and AA. This outcome might be attributed to relative basicity of the secondary amine group present on the piperazine ring and relative acidity of the hydrogen present on the carboxylic acid substituent of the co-formers asides from pKa rule. Here it is also important to remind that the secondary amine present on the piperazine of SPX does not have steric hindrance; therefore, it is relatively easier for the reaction to proceed. Furthermore, all the co-formers tested in this study, have additional electron donating groups such as $–NH_2$ and –OH as a substituent on the benzene ring, which might decrease the relative acidity of the hydrogen present on the carboxylic moiety of the co-former. However, the salt formation was successful. The only structural difference between co-formers relies on either in the position or additional hydroxyl group, in the case of 4-ASA. The formation of salt between SPX and AA is not restricted due to the ortho position of the $–NH_2$ substituent; instead, this moiety contributes to the intermolecular connection between SPX and AA molecules.

One of the most challenging aspects of this study was in terms of the control of the synthetic procedures to obtain pure phases, specifically in case of multicomponent forms with SPX and 4-ASA. The control over the crystal form was unsuccessful by the application of slow evaporation method. Indeed, the crystals of **SPX:4ASA Forms II** and **III** were obtained with the same experimental conditions using the slow evaporation method. In this regard, it can be stated that the pure phase formation of SPX and 4-ASA salts can hardly be achieved by slow evaporation. However, the use of mechanochemistry was more powerful under specific conditions. This outcome highlights the strength of mechanochemistry in the co-crystal and salt screening of Sparfloxacin.

One of the desirable outcomes of multicomponent screening of an API is to alter and improve the physicochemical properties and solubility behaviour is the foremost of an consideration. Even though the method applied throughout this study is an empirical method and further studies are required for more accurate deduction, the new pharmaceutical forms obtained in this study clearly augment the solubility of the API. Additionally, it is needed to note there that the stability is also another consideration for pharmaceutical APIs. Within this study, it is also shown that the new multicomponent forms of SPX are stable at least for 4 weeks under a 78% humidity atmosphere.

Bringing all together, it can be stated that SPX requires improvement in its biological activity as well as physicochemical properties. By the help of crystal engineering principle and combining the API with suitable co-formers within just a single crystal lattice, it is possible to improve its solubility profile. What is more important is that boosting its antimicrobial activity can be achieved, allowing a reduction the oral dose needed by simply combining the API with other antibiotics, such as 4-ASA and NA. More

importantly, the new dual antibiotic multicomponent forms with SPX and 4ASA can be a superior alternative treatment for tuberculosis. To confirm its viability as a pharmaceutical compound, cytotoxicity, and antimicrobial activity tests are planned for a near future.

References

1. G. R. Desiraju and G. W. Parshall, *Materials science monographs*, 1989, **54**.
2. G. Schmidt, *Pure and Applied Chemistry*, 1971, **27**, 647-678.
3. A. Nangia, *Journal of chemical sciences*, 2010, **122**, 295-310.
4. J. Lehn, *Pure and applied Chemistry*, 1978, **50**, 871-892.
5. G. R. Desiraju, *Angewandte Chemie International Edition in English*, 1995, **34**, 2311-2327.
6. J. D. Dunitz, *Pure and applied chemistry*, 1991, **63**, 177-185.
7. E. J. Corey, *Pure and Applied chemistry*, 1967, **14**, 19-38.
8. E. Corey, *Chemical Society Reviews*, 1988, **17**, 111-133.
9. *Cambridge Structural Database* https://www.ccdc.cam.ac.uk/ (accessed June 15, 2019).
10. S. Domingos, V. André, S. Quaresma, I. C. Martins, M. F. Minas da Piedade and M. T. Duarte, *Journal of Pharmacy and Pharmacology*, 2015, **67**, 830-846.
11. M. C. Etter, *Accounts of Chemical Research*, 1990, **23**, 120-126.
12. M. C. Etter, J. C. MacDonald and J. Bernstein, *Acta Crystallographica Section B: Structural Science*, 1990, **46**, 256-262.
13. J. W. Mullin, *Crystallization*, Elsevier, 2001.
14. D. Guranda and G. Deeva, *Pharm Chem J*, 2010, **44**, 22-28.
15. A. M. Healy, Z. A. Worku, D. Kumar and A. M. Madi, *Advanced drug delivery reviews*, 2017, **117**, 25-46.
16. D. Gupta, D. Bhatia, V. Dave, V. Sutariya and S. Varghese Gupta, *Molecules*, 2018, **23**, 1719.
17. U. D. o. Health, H. Services, Food and D. Administration, *Center for Drug Evaluation and Research (CDER), Silver Spring, US*, 2018.
18. A. Mukherjee, *Crystal Growth & Design*, 2015, **15**, 3076-3085.
19. N. Schultheiss and A. Newman, *Crystal growth and design*, 2009, **9**, 2950-2967.
20. W. Jones, W. S. Motherwell and A. V. Trask, *MRS bulletin*, 2006, **31**, 875-879.
21. P. H. Stahl and C. G. Wermuth, *Chem. Int*, 2002, **24**, 21.
22. F. Wöhler, *Untersuchungen über das Chinon*, 1844.
23. P. Pfeiffer, *Organische Molekülverbindungen*, F. Enke, 1922.
24. A. Karagianni, M. Malamatari and K. Kachrimanis, *Pharmaceutics*, 2018, **10**, 18.
25. I. Miroshnyk, S. Mirza and N. Sandler, *Expert opinion on drug delivery*, 2009, **6**, 333-341.
26. N. Qiao, M. Li, W. Schlindwein, N. Malek, A. Davies and G. Trappitt, *International journal of pharmaceutics*, 2011, **419**, 1-11.
27. M. Karimi-Jafari, L. Padrela, G. M. Walker and D. M. Croker, *Crystal Growth & Design*, 2018, **18**, 6370-6387.

28. A. Jayasankar, L. S. Reddy, S. J. Bethune and N. Rodríguez-Hornedo, *Crystal Growth and Design*, 2009, **9**, 889-897.

29. J.-L. Do and T. Friščić, *ACS central science*, 2016, **3**, 13-19.

30. Sparfloxacin Drug Bank, https://www.drugbank.ca/drugs/DB01208 (accessed June 15, 2019).

31. M. I. Andersson and A. P. MacGowan, *Journal of Antimicrobial Chemotherapy*, 2003, **51**, 1-11.

32. B. Suh and B. Lorber, *Medical Clinics of North America*, 1995, **79**, 869-894.

33. J. S. Wolfson and D. C. Hooper, *Antimicrobial agents and Chemotherapy*, 1985, **28**, 581.

34. T. Miyamoto, J.-i. Matsumoto, K. Chiba, H. Egawa, K. Shibamori, A. Minamida, Y. Nishimura, H. Okada, M. Kataoka and M. Fujita, *Journal of medicinal chemistry*, 1990, **33**, 1645-1656.

35. S. Nakamura, A. Minami, K. Nakata, N. Kurobe, K. Kouno, Y. Sakaguchi, S. Kashimoto, H. Yoshida, T. Kojima and T. Ohue, *Antimicrobial agents and chemotherapy*, 1989, **33**, 1167-1173.

36. C. Pierfitte, R. J. Royer, N. Moore and B. Bégaud, *British journal of clinical pharmacology*, 2000, **49**, 609-612.

37. N. K. Gibbs, in *Comprehensive Series in Photosciences*, Elsevier, 2001, vol. 3, pp. 337-356.

38. K. Outterson, J. H. Powers, E. Seoane-Vazquez, R. Rodriguez-Monguio and A. S. Kesselheim, *The Journal of Law, Medicine & Ethics*, 2013, **41**, 688-696.

39. T. Miyamoto, J. Matsumoto, K. Chiba, H. Egawa, K. Shibamori, A. Minamida, Y. Nishimura, H. Okada and M. Kataoka, *Journal of Medicinal Chemistry*, 1990, **33**, 1645-1656.

40. A. Sivalakshmidevi, K. Vyas and G. Om Reddy, *Acta Crystallographica Section C: Crystal Structure Communications*, 2000, **56**, iuc0000046-e0000116.

41. A. Llinàs, J. C. Burley, T. J. Prior, R. C. Glen and J. M. Goodman, *Crystal Growth and Design*, 2008, **8**, 114-118.

42. D. Shingnapurkar, R. Butcher, Z. Afrasiabi, E. Sinn, F. Ahmed, F. Sarkar and S. Padhye, *Inorganic Chemistry Communications*, 2007, **10**, 459-462.

43. A. Vasiliev and N. Golovnev, *Journal of Structural Chemistry*, 2015, **56**, 907-911.

44. E. K. Efthimiadou, Y. Sanakis, C. P. Raptopoulou, A. Karaliota, N. Katsaros and G. Psomas, *Bioorganic & medicinal chemistry letters*, 2006, **16**, 3864-3867.

45. A. Gunnam, K. Suresh, R. Ganduri and A. Nangia, *Chemical Communications*, 2016, **52**, 12610-12613.

46. Antranilic acid drug bank, https://www.drugbank.ca/drugs/DB04166, (accessed June 15, 2019).

47. 3-aminobenzoic acid http://www.hmdb.ca/metabolites/HMDB0001891 (accessed 15 June, 2019).

48. https://www.drugbank.ca/drugs/DB00233 (accessed June 16, 2019).

49. M. Pudipeddi and A. T. Serajuddin, *Journal of pharmaceutical sciences*, 2005, **94**, 929-939.

50. M. Tyers and G. D. Wright, *Nature Reviews Microbiology*, 2019, 1.

51. M. Djalo, V. Andre , M. Teresa Duarte unpublished work.